Distribution Category:
Materials (UC-25)

ANL-75-66

ARGONNE NATIONAL LABORATORY
9700 South Cass Avenue
Argonne, Illinois 60439

FACIES OF ION BOMBARDED SURFACES OF BRITTLE MATERIALS

by

William Primak

Solid State Science Division

December 1975

Disclaimer: This is a preliminary report and conclusions may be modified as further results are accumulated.

PREFACE

For several years now, it has seemed that feasibility of a fusion reactor will be demonstrated in the near future. Thus, concern over materials problems for such reactors has arisen. At first these concerns were directed toward the behavior of metals, but then designs were developed in which non-metallic surfaces would be exposed to plasma or to ion beams. Materials being considered were among those which had been investigated in our laboratory in single crystal form over a period of several decades. Since we had begun studying polycrystalline surfaces, it became appropriate to investigate typical commercial materials which might be employed. In the course of investigating the swelling and reflectivity following ion bombardment, new insights into the mechanism of radiation blistering of brittle materials were obtained. Since the information may prove valuable in controlling surface deterioration of such materials in practical applications, and to fusion devices or accelerators, this report has been prepared to disseminate the information more promptly than is possible through customary channels of scientific publication.

In this report, blistering refers to the development of gas pockets which cause spheroidal or irregular protuberances on the surface. Typically, the lower internal surface of a blister is quite flat. With the ions and energies used in the present study, the blisters can be seen at magnifications obtained with optical microscopes. Gas pockets small enough and sufficiently far from the surface that they do not cause noticeable surface deformation, nor can be seen even at very high magnification in the optical microscope, will be referred to as pores and a distribution of them as porosity.

This report gives our findings. The material which is usually antecedant in a scientific paper: introduction, and experimental methods, will be found in the appendices.

This laboratory had originally been concerned with radiation effects[1-6] encountered in the graphite moderated nuclear reactors. In the course of attempting to separate effects caused by various radiations and to determine the energy dissipated during the slowing down of energetic atoms by ionization and scattering, much of the program was shifted to the use of various accelerators;[7] and most recently much of the work has been with ion bombardment. It was in the early phases of these investigations that exfoliation of the bombarded layer was observed[8] and that radiation blistering[9] was discovered in our laboratory, in some of the very materials now of interest in the CTR program.

Some of the materials employed in the present study were chosen because of current plans for their application (alumina, silicon nitride, silicon carbide, SCB glasses), and others were included to develop information about the general nature of the phenomena. The materials thus far investigated, arranged in groups which show similarities in behavior, are:

BLANK PAGE

1. Quartz

2. Glasses

   a. vitreous silica, Pyrex glass
   b. borosilicate crown, crown, light barium crown, SCB
   c. dense barium crown
   d. flint glasses

3. Carbides, borides: SiC, B_4C, TiB_2

4. Oxides, nitrides

   a. magnorite, sapphire, spinel (original studies of single crystals, 1962-1966)
   b. compacts: Al_2O_3, Si_3N_4, ZrO_2, $BaTiO_3$.

Examination of several forms of carbon has just begun, and the glass used for Raschig rings employed for neutron absorption in solutions of fissionable materials is also being studied. These materials are being subjected to ion bombardment by protons, deuterons, and helium ions, mainly 140 keV. The effects have little dependence on energy. The ranges of the ions at these energies are convenient for our observations of swelling, blistering, surface deformation, and surface ablation.

The course of these investigations has been determined as much by the availability of the accelerator as by the results of the observations so that usually several divergent lines of investigation have been pursued simultaneously. Such was the case here. It was long understood that the blistering was associated with the permeability of the material to the gas. The interest in the SCB glasses for nuclear and possibly CTR application offered an opportunity to study glasses in general because their permeability was known to be a function of composition. Quartz had been under investigation for a long time and had been irradiated a number of years ago. Investigation of it was resumed upon developing more precise methods of measurement. Investigation of the crystalline materials began upon the development of techniques applicable to ceramic bodies. These several investigations converged when it was found that the bodies which were opaque in the visible gave chromatic fringes in reflection in the infra-red and lead to the formulation of the hypothesis of the microporous layer. With the presentation of this hypothesis, we have gone through a cycle from the original hypothesis that ion bombardment of silicon caused a change in refractive index, then to the hypothesis that a discrete gaseous layer was involved, and now to the concept of a mixed medium of variable effective refractive index.

The accelerator was operated by Allan C. Youngs who performed all of the bombardments and who obtained the dose data.

Emmet Monahan assisted in the later stages of the investigations. He obtained some of the reflectivity data and prepared some of the photographic material used for the interferometric measurements.

Acknowledgment must also be made to the former Director of the Solid State Science Division, O. C. Simpson, and to the present Director, D. L. Price, and Assistant Director, D. Y. Smith, for encouraging and supporting these investigations.

William Primak
December 1975

TABLE OF CONTENTS

BLANK PAGE

LIST OF FIGURES

FACIES OF ION BOMBARDED SURFACES OF BRITTLE MATERIALS

by

William Primak

ABSTRACT

A number of materials were subjected to ion bombardment by protons, deuterons, and helium ions for the purpose of determining the surface deterioration under such treatment. The work was stimulated by current interests in the CTR materials programs. Some materials were chosen because of current plans for their application (alumina, silicon nitride, silicon carbide, SCB glasses) and others were included in the investigation to develop information about the general nature of the phenomena.

The materials which have thus far been investigated are arranged in groups which show similar behavior:

1. Quartz

2. Glasses

   a. vitreous silica, Pyrex glass
   b. borosilicate crown, crown, light barium crown
   c. dense barium crown
   d. flint glasses

3. Carbides, borides: SiC, B_4C, TiB_2

4. Oxides, nitrides:

   a. magnorite, sapphire, spinel (original studies of single crystals, 1962-1966)
   b. Compacts: Al_2O_3, Si_3N_4, ZrO_2, $BaTiO_3$

5. Miscellaneous graphite, $LiNbO_3$, copper

The observations were of growth, reflectivity as a function of wavelength, microscopic examination for blistering, surface ablation, etc., blister and blister shell dimensions, and swelling as seen in surface deformation.

Calculations were made of (1) the effects of (a) a layer, of (b) the gradual transformation of a layer, and of (c) the introduction of a gas, on the reflectivity, and (2) dimensional and mechanical changes associated with blister formation.

Tentatively the following conclusions have been reached:

1. Radiation blistering is not a primary process.

2. Observations of blister formation and exfoliation cannot be used to calculate the surface ablation rate associated with this process.

3. The primary process is the development of a microporous layer which causes swelling.

4. The development of visible blisters is caused by fracturing in this layer and may occur during the bombardment, or in some cases, much later, on storage.

5. There is no evidence of extreme gas pressures in the blisters.

6. The blisters do not develop by yielding under high gas pressure. They develop because of the transverse stresses associated with a radiation expansion or the microporosity.

7. When blisters develop, they may be stable under continued bombardment for a dose many times that at which they formed. Evidently the energy of the ions is dissipated in the blister shell, and the gas escapes through fissures in the surface.

8. The swelling is a better index of the effects than is the blistering, and it must be associated in most cases with permeability to the gas. Behavior with protons and deuterons is similar, with helium different. In the classification above, all but quartz and Class 2a are impervious to hydrogen and deuterium; only 2C, 3, and 4 are impervious to helium.

Quartz is a special case which shows swelling caused by conversion to a vitreous product of much lower density, but no porosity. For the others, most of the swelling and surface growth is caused by porosity.

It seems likely that the rate of surface ablation by the blistering process can be reduced by initial porosity or by initial or subsequent surface fissuring. However, for impervious materials, surface damage by the introduction of porosity would continue.

VISIBLE CHANGES

On most of the materials, the bombarded areas were distinguishable. The causes were various: coating, coloration, interference effects, change in reflectivity, blistering, exfoliation, fracture, spallation, change in surface properties among them. In some cases where growth caused a sharp step, optical phenomena associated with the edge made it visible. Causes associated with chemical change, coloration, and alteration of surface properties are treated here.

A number of the glasses showed a deposit of crystalline particles or liquid droplets on the irradiated areas, usually arranged in interesting patterns, hence called "decoration",[10] after bombardment. This phenomenon was noted by Hines[11] who attributed it to the selective sputtering of alkali atoms of the glass. The phenomenon can usually be observed by a dose of 15 mC/cm^2 of incident ions, and the quantity of material seems much more than could be formed by sputtering. It seems rather to be caused by alkali migration under ion bombardment,[10] followed by reaction with water and carbon dioxide from the atmosphere. Some of the glasses became redecorated after the original decoration was removed but glasses which did not show post-irradiation decoration, like Pyrex, were decorated after the ion bombardment.

Of the crystalline materials, the only ones for which definite evidence of change in chemical composition was noted were lithium niobate and silicon carbide. Lithium niobate showed the decoration by alkali migration.[12] The irradiated areas of silicon carbide were coated with a soot-like deposit which could be removed by rubbing a tungsten or other smooth metal needle on the surface.

Few of the materials developed sufficient color to be visible in the thin layers affected to show a noticeable true coloration apart from interference effects. Exceptions were the flint glasses[13] and silicon carbide crystals. The silicon carbide crystals were originally a light green color. All bombarded areas (proton, deuteron, or helium ion bombardments) turned black. The zirconia specimens were originally a yellow color. Specimens bombarded with deuterons, helium ions, and neon ions were studied. The helium ion bombarded areas turned golden, and the neon bombarded areas turned darker; but these colorations are suspected to be interference effects. The darkening by deuterons seems to be an intense absorption.

The surface properties of the bombarded glasses are altered. After permitting water to flow over them, it will drain off the unbombarded area, but drops will cling to the bombarded areas. This effect has been attributed to the alkali migration.[10]

GROWTH OF GLASSES

Many of the bombarded areas become elevated above the rest of the surface. Interferograms of such surfaces have been published, as have curves for growth as a function of dose.[14] Growth curves for crystalline materials are presented following the sections on blistering and porosity. Typical growth curves for glasses are shown in Fig. 1 and a summary of the growth data are given in Table I.

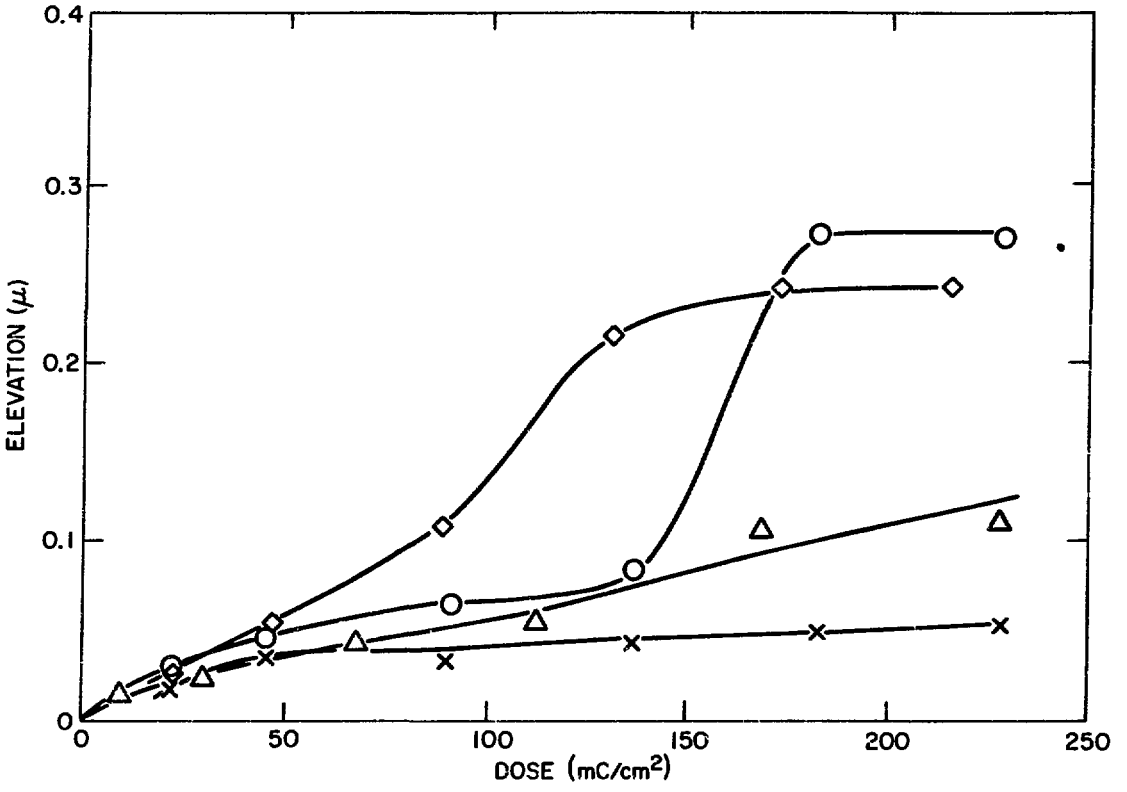

Fig. 1: Typical growth curves for areas of glasses bombarded with 140 keV ions. Circles: protons on C-1 glass--gentle rise followed by abrupt rise ("breakaway"); X's: deuterons on C-1 glass--low saturation; diamonds: deuterons on BK-7--high saturation; triangles: protons on LF-2--rising.

Table I. Growth of 140 keV Ion Bombarded Areas of Glasses

Glass	Ion	Character as Function of Dose	Height @ Dose (μ)	(mC/cm^2)	Breakaway[a] Dose
Pyrex	H^+	Nil			
	D^+	Very Small			
	He^+	Nil			
BK-7	H^+	Gentle Rise	0.08	132	
	D^+	High Saturation	0.24	168	
	He^+	Nil			
C-1	H^+	Gentle Rise	0.3	132	138
	D^+	Low Saturation	0.2	240	
	He^+	Nil			
TF	H^+	Low Saturation	0.2	228	
	D^+	Gentle Rise	0.45	180	
	He^+	Nil			
LBC-1	H^+	Low Saturation	0.2	228	
	D^+	Low Saturation	0.2	228	
	He^+	Nil			
BAK-5	H^+	Low Saturation	0.2	228	
	D^+	Low Saturation	0.2	228	
	He^+	Nil			
LBC-2	H^+	Low Saturation	0.2	90	120
	D^+	Low Saturation	0.2	90	120
	He^+	Nil			
SCB	H^+	Rising	0.5	150	156
	D^+	Rising	0.5	150	156
	He^+				
DBC-5	H^+	Rising	0.7	180	
	D^+	Rising	0.6	132	
	He^+	Low Saturation	0.1	24	24
LF-2	H^+	Rising	0.4	228	
	D^+	Rising	0.7	228	
	He^+	Nil			
DF-3	H^+	Rising	0.45	228	
	D^+	Rising	0.55	228	
	He^+	Nil			

[a]Dose at which curve shows a sudden rise usually to about 0.27 μ; see Fig. 1. If no value is given, breakaway did not occur over the dose range investigated, usually to 228 mC/cm^2, but in some cases to 360 mC/cm^2.

REFLECTIVITY

The reflectivity changes usually involve interference effects in the thin bombarded layers and are wavenumber dependent; in the spectroscope, reflected white light gives channelled spectra. We refer to fringes observed on varying wavelength as chromatic fringes. These chromatic fringes show secondary interference effects (i.e., other periods than the primary one) indicating a non-uniformity in depth. The primary period of the chromatic fringes gives the thickness of a surface layer, whether it is a blister shell, or whether it results from a change in refractive index. Several materials which were too absorbing in the visible region (or which for other reasons) did not show chromatic fringes in the visible region, showed excellent fringes in the near infra-red. Such were boron carbide and silicon carbide, and some of the glasses. Layer thicknesses were calculated from the chromatic fringes by the formula:

$$1/t = 2N \cos\theta(\Delta\omega/\Delta n)$$

where t is the layer thickness in microns, N is the refractive index, θ is the angle of incidence, and $\Delta\omega/\Delta n$ is the fringe spacing in reciprocal microns. Results are given in Table II.

The absolute value of the reflectivity and the amplitudes of the chromatic fringes are more difficult to interpret. The experimental data for quartz seemed particularly simple, and therefore it is considered first. The reflectivity for a homogeneous film on a substrate lies below the substrate reflectivity when the film has a refractive index lower than that of the substrate and above the substrate reflectivity when the film refractive index is greater than that of the substrate. On the basis of approximate calculations for the system two films on a substrate, Hines and Arndt[15] pointed out that this is no longer true when the refractive index of the film is non-uniform. Exact calculations for the system two films on a substrate are readily performed with modern computational equipment. The case considered (Fig.2D) was the two layer system in which a fixed thickness of the substrate was regarded as a film and a portion, α, of this thickness was transformed to a material of lower refractive index and density. The refractive indices and densities were those of quartz transformed to irradiated vitreous silica.[16] The refractive index of quartz was taken as $1.5324 + 0.00407\ \lambda^{-2}$ and that of vitreous material as $1.4586 + 0.00355\ \lambda^{-2}$. The thickness of the completely vitrified layer was taken as 1.89 μ which would have been formed from 1.57 μ of original quartz, the range of 140 keV deuterons. The thicknesses of the respective layers are then:

$$d_1 = (1 - \alpha)T; \quad d_2 = \alpha T(2.6481/2.2023).$$

Figure 2A compares the early stages of transformation with the reflectivity of quartz and the completely vitrified layer on the quartz. Figure 2B gives the reflectivity for the intermediate stages of transformation, and Fig. 2C are the results for the final stages of the transformation. The two horizontal lines are the reflectivities of quartz and the vitreous material, $(N - 1)^2/(N + 1)^2$. From α approximately 0.03--0.97, the chromatic fringes lie about (i.e., partly above, partly below) the reflectivity of the substrate. It is therefore concluded that even a very small non-uniformity of the refractive index will cause this effect. In all of the cases there was a decrease in refractive index, yet the chromatic fringe maxima were above the substrate reflectivity for most of the transformation; and at stages of the

Table II. Layer thickness from chromatic fringe spacing.*

MTL	Density	Refractive Index	Notes	H^+		D^+		He^+	
				Fringe Spacing (1/μ)	Thickness (μ)	Fringe Spacing (1/μ)	Thickness (μ)	Fringe Spacing (1/μ)	Thickness (μ)
Quartz	2.20	1.48	Vitrified	0.235	1.53	0.19	1.89	0.365	0.99
Pyrex	2.28	1.472		0.26	1.39	0.20	1.81	0.375	0.97
BK-7	2.42	1.516		0.25	1.36	0.21	1.62	0.42	0.81
C-1	2.57	1.521		0.26	1.35	0.21	1.67	0.415	0.84
TF	2.70	1.527		0.23	1.51	0.20	1.74		
LBC-1	2.85	1.541		0.23	1.50	0.19	1.82	0.42	0.82
LBC-2	3.20	1.573		0.24	1.41	0.20	1.69		
SCB		1.524							
SCB		1.556							
DBC-5	3.68	1.636						0.49	0.69
LF-2	3.05	1.578		0.23	1.47	0.20	1.69		
			80 keV	0.33	1.02				
DF-1	3.45	1.604		0.23	1.44	0.20	1.66		
SiC X1	3.21	2.61							
			100 keV						
SiC I	3.15	2.61			1.14		1.50		0.93
SiC A	3.15	2.61		0.17	1.20	0.13	1.55	0.21	0.97
B_4C	2.45	1.9			1.47		1.72		0.95
Si_3N_4	3.15	2.0		0.26	1.03	0.20	1.32	0.37	0.72
ZrO_2	5.6	2.17			0.91		1.11		0.53
$BaTiO_3$	6.	2.4	Alsimag	0.34					0.62
Lucalox	4.	1.76		0.31	0.94				
Al_2O_3	4.	1.76	Ceralloy	0.31	0.94				
Al_2O_3	4.	1.76	Coors	0.31	0.93				

*Missing items either because suitable specimens for measurement were not available or because data had not yet been obtained and processed when this report went to press.

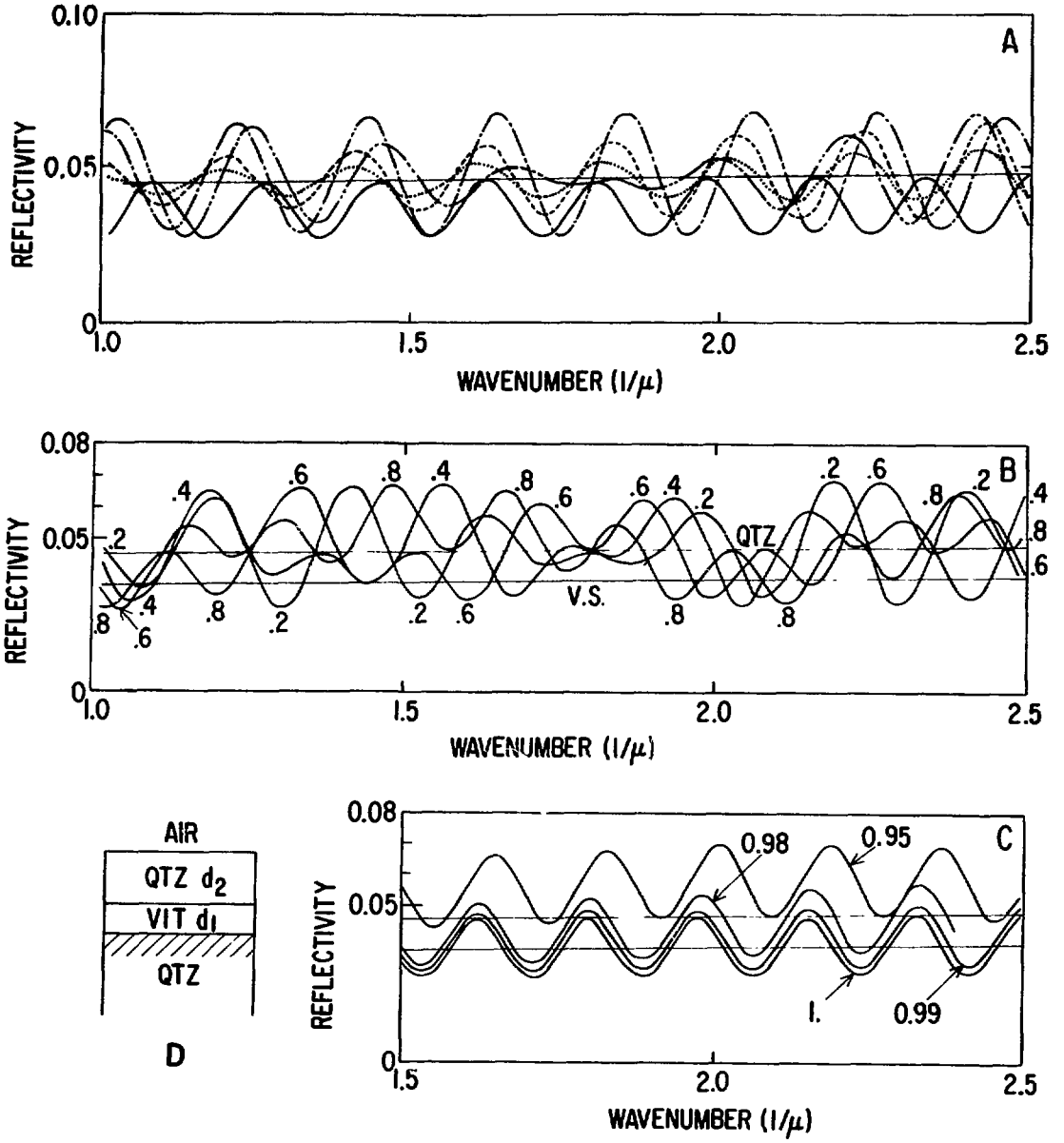

Fig. 2: Calculated reflectivity of a layer of quartz being vitrified.
A. Early stages of the transformation; solid line reflectivity of quartz; solid curve completely vitrified, $\alpha = 1$; dotted, $\alpha = 0.01$; dashed, $\alpha = 0.02$, dot-dash, $\alpha = 0.05$; dash-double dot, $\alpha = 0.1$.
B. Reflectivities for the intermediate stages of transformation, α 0.2 to 0.8. The two lines are the respective reflectivities for quartz and vitrified quartz.
C. Final stages of transformation, α 0.95 to 1.0. The two lines are the respective reflectivities of quartz and vitrified quartz.
D. The system of two quartz films of differing density on a quartz substrate.

transformation, even the minima lay above the substrate reflectivity. Therefore, this condition cannot be taken as proof that an increase in refractive index is occurring.

When a gas layer is introduced, the chromatic fringe amplitude increases markedly, and high reflectivities are found at some wavelengths. In the absence of refractive index changes, very thin layers can be detected, less than 0.001 μ. From the data plotted in Fig. 3, despite the refractive index

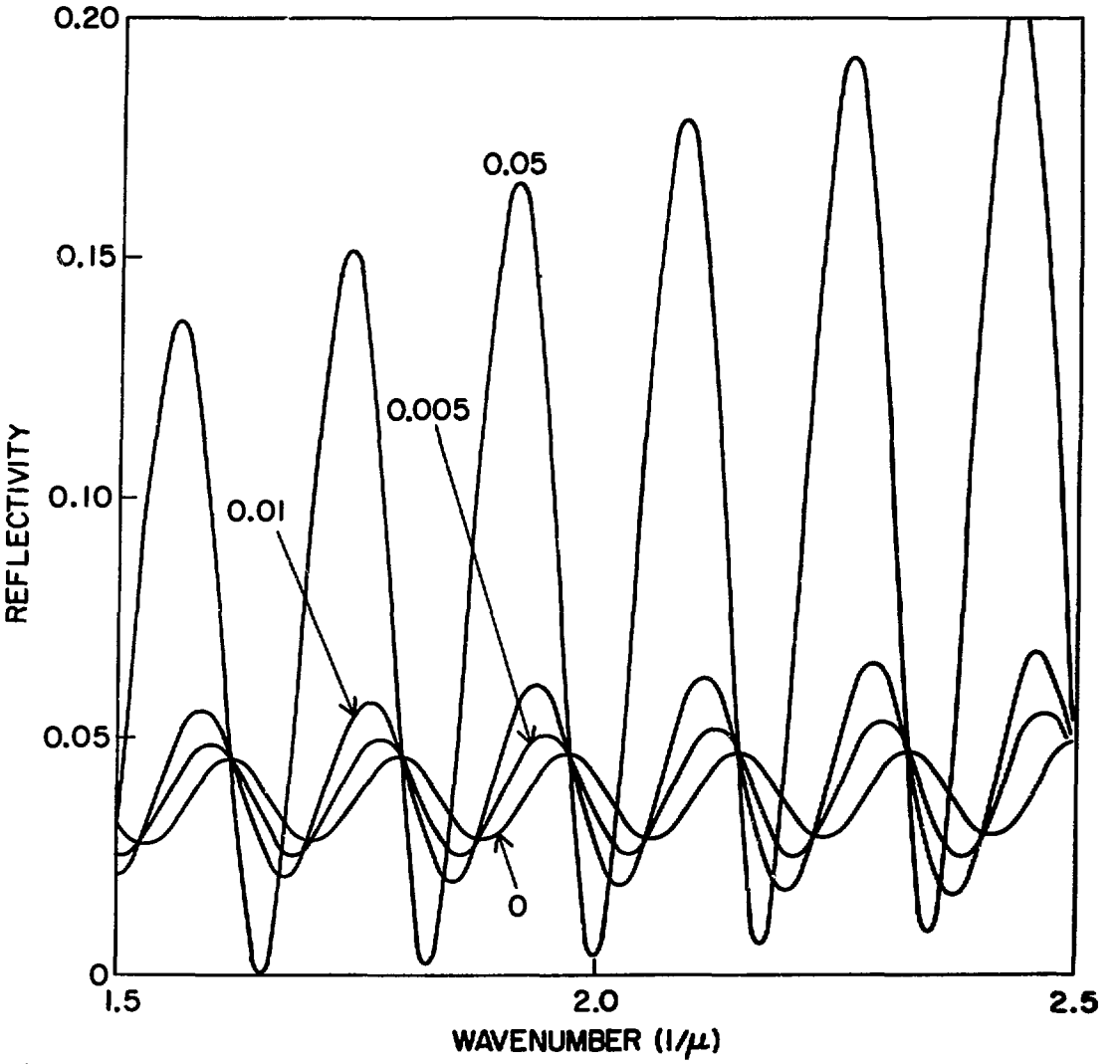

Fig. 3: Reflectivity calculated for quartz covered with a 1.57 μ layer of vitrified quartz with an intervening gas layer of the thickness (in microns) given on the respective curves.

change which also introduces chromatic fringes, a layer a few millimicrons thick could be detected. Reflectivities will rise to some 30% when the layer thickness is about $\lambda/4$, but this could not be accommodated in the figure. The periods of the chromatic fringes do not change and correspond to the shell thickness. In this case where the shell is of constant refractive index and thickness and in which the layer is of constant refractive index, the fringes intersect in each period at the shell reflectivity. It will be seen that none of the experimental curves have this property, indicating changes in optical path in the shell or a varying refractive index in the intermediate layer.

Measurements of the reflectivity of deuteron bombarded quartz are shown in Fig. 4. Results for proton bombarded quartz were similar. It is seen that the behavior corresponds to the case of a change in refractive index rather than the introduction of a gas layer. The amplitude of the fringes does not reach that calculated, and this is attributed to the gradual change in refractive index with depth in contrast to the abrupt changes used in the calculations. The important point is that the fringe maxima do not rise as the bombardment is extended; they fall to a value hardly above that of unirradiated quartz. It must therefore be concluded that gas segregation does not occur; that the vitreous layer must be pervious to the gases.

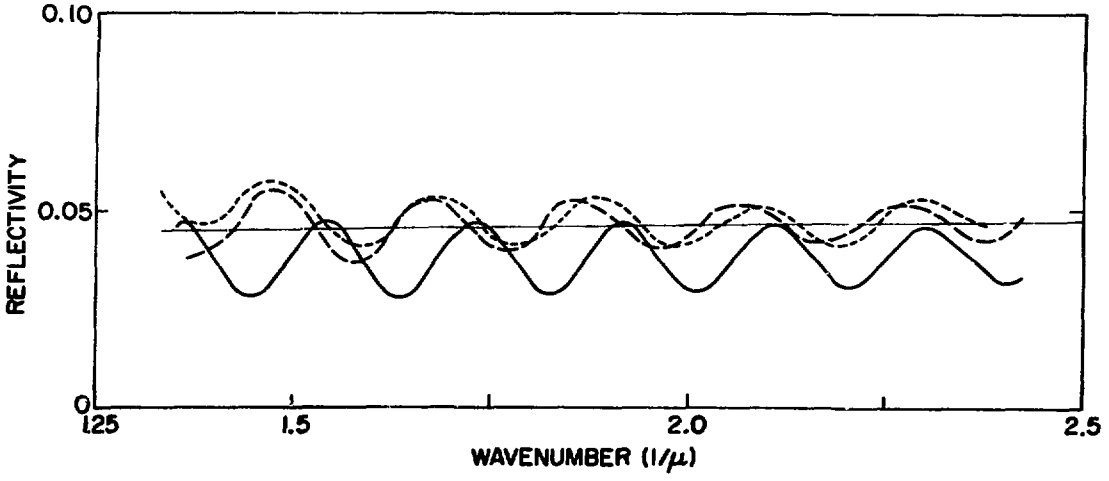

Fig. 4: Experimental measurements of the reflectivity of 140 keV deuteron bombarded quartz relative to unirradiated quartz scaled to the reflectivity assumed in Figs. 2 and 3. Plate orientation parallel to the optic axis. Solid line, assumed value for unirradiated quartz; solid curve, 240 mC/cm^2; dotted line, 3 mC/cm^2; dashed line, 12 mC/cm^2.

In the cases of the transparent crystals like sapphire, spinel, and magnorite, interpretation of the chromatic fringes was unequivocal because the fringe amplitudes rose to high values and blisters visible under the microscope appeared. Areas showing high reflectivity showed a "graininess" which could be correlated with a graininess of the substrate viewed in

interference when the blister shell broke away. For a number of the glasses which showed appreciable growth of the bombarded areas, for which chromatic fringes of considerable amplitude developed, and from which, eventually, the bombarded layer broke away, blisters visible under the microscope did not appear. Graininess was not seen in the highly reflecting areas. The fringe amplitudes did not develop quickly with dose as in the case of quartz. To begin with, the chromatic fringes were below the substrate reflectivity, but as the dose was increased, the reflectivity oscillated about the substrate reflectivity and grew until the fringe amplitude was approximately 2/3 of the substrate reflectivity. Maximum reflectivities were some 6-7%. While, for these materials, the reflectivities were probably too large to be accounted for by changes in refractive index, it was far below 0.2 to 0.3 that should have been reached if a gas layer were continuing to grow. When the bombarded layer broke away, the reflectivity of the new surface was so low it was difficult to obtain enough light to observe fringes on this surface. In the cases of the crystals, although this underlying surface did not have as high a reflectivity as the original polished surfaces, it was sufficiently great that there was no difficulty in using the surface for interferometric measurement. It is therefore concluded that in the case of these glasses a sub-microscopic porosity develops, probably with variation in depth greater than in the case of the crystals. Such a layer should be a poorer reflector at shorter wavelengths, and indeed fringes of greater amplitude are found in the infra-red above 1 μ than in the visible.

BLISTERING

Evidence of gas segregation following ion bombardment with gas ions of micron range is readily observed in transparent crystals on examination in monochromatic vertical illumination under the microscope. It is less readily observed in opaque materials or ceramic bodies, particularly when the blisters are small. However, evidence of gas segregation was found for most of the crystalline materials examined here. The results of microscopic examination are summarized in Table III.

Individual blisters were examined at high magnification in the Zeiss interference microscope. The diameters and heights of some of the largest blisters were measured and typical blisters were photographed. The measurements are given in Table III and typical examples of the blistering are shown in Fig. 5. When the monochromatic fringes formed by the blister cavity were visible, the height (in fringes) was not appreciably different from the external height (in fringes) viewed in a Twyman-Green configuration.

If it is assumed that the blister is a portion of a sphere,[17] the following quantities are readily calculated from the diameter L and the height a: the radius of curvature r, the volume V, and the linear expansion $\Delta L/L$ of the shell in forming the blister. If it is assumed that all of the gas incident on the blister is within it, the pressure P can now be calculated from the foregoing and the dose D. The shell thickness t is known from the chromatic fringes and the index of refraction of the material. It is now possible to calculate a yield modulus Y. Thus,

Table III. Initial appearance of blisters, largest visible (140 keV ions unless otherwise noted).

Material	Ion	American Optical Microscope, 8 mm objective			Zeiss interferences Microscope 600x or 250x		
		Blister Diameter (μ)	Height (μ)	Dose (mC/cm^2)	Blister Diameter (μ)	Height (μ)	Dose (mC/cm^2)
SiC (X1)	H	6-15	0.54	364	20		
	D(100)	No					
	He	3-10	0.13-1.1	364	9-14		
SiC I	H	16-23			9-19	1.1-2.6	152
	D	23-37			25-33	2.7-4.3	279
	He	7			4	0.9	152
SiC A	H	11					
	D	No					
	He	No					
Si_3N_4	H	No			9	0.3-8	137
	D	No			3-4	0.25	182
	He	No			1.5	0.22	184
B_4C	H	100 x 400	∿4.1		64-74	1.3-2.2	152
	D	100 x 400	Exfol	144	25	0.31	182
	He	11			8.4	0.31	137
TiB_2	H	14-35		46	18	0.7	46
	D	20-50		11	15	0.38	91
	He	10-50		137	12.6	0.62	91
$BaTiO_3$	He	No					
ZrO_2	H	4.5-20	1.0	60			
	D	5-40	1.2	91			
	He	7-12	0.9	46			
	Ne	1-2	0.2	46			
Lucalox	H	2.3-11.5	0.2	144	7.3	0.54	144
	He	11.5-16	0.8	72	9	0.43	72
Al_2O_3, Coors	H	4.5-11.5	0.2-0.7				
	D	2.5-11.5	0.2				
	He	2-9	0.4				
Al_2O_3, Ceralloy	H	5-25		61	23	0.5	61
	D	11-30		137	31	0.76	137
	He	No			4	0.3	228

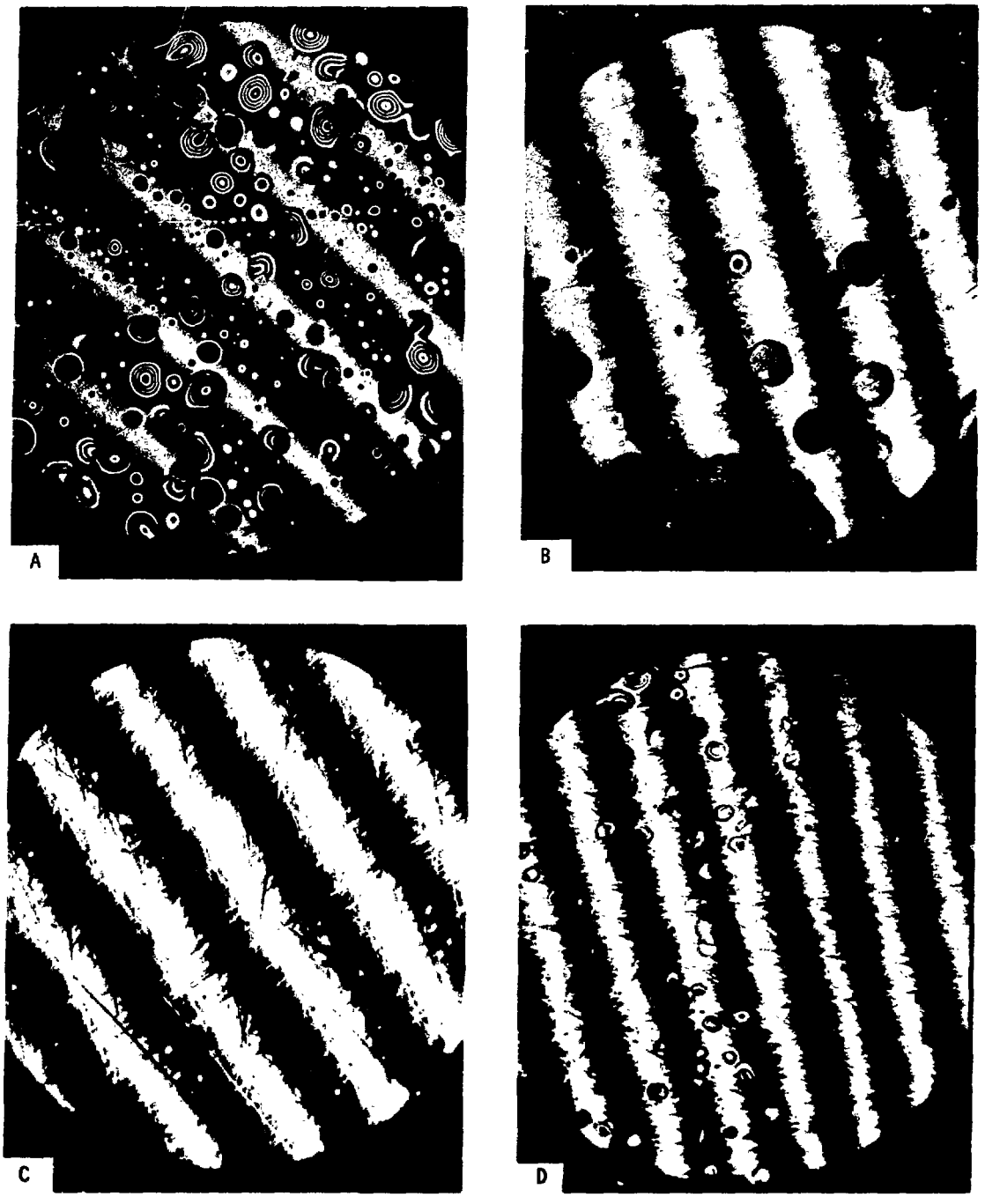
A
B
C
D

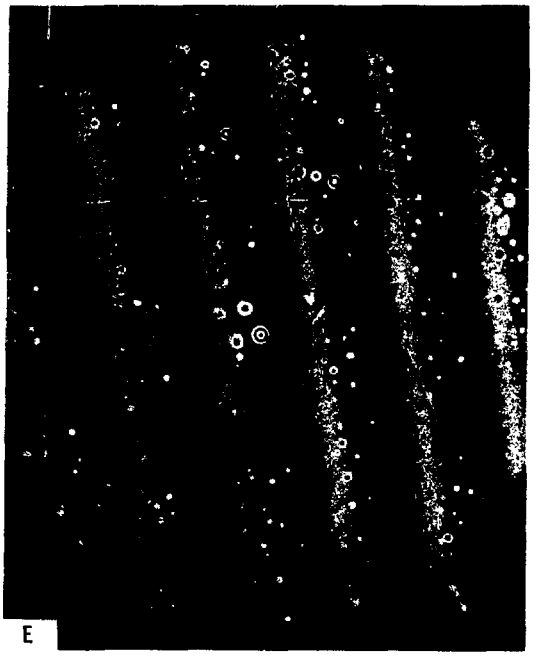

E

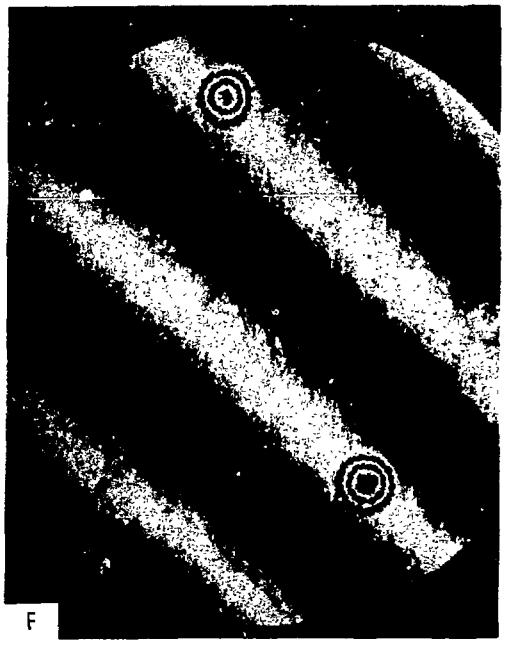

F

G

H


J


K

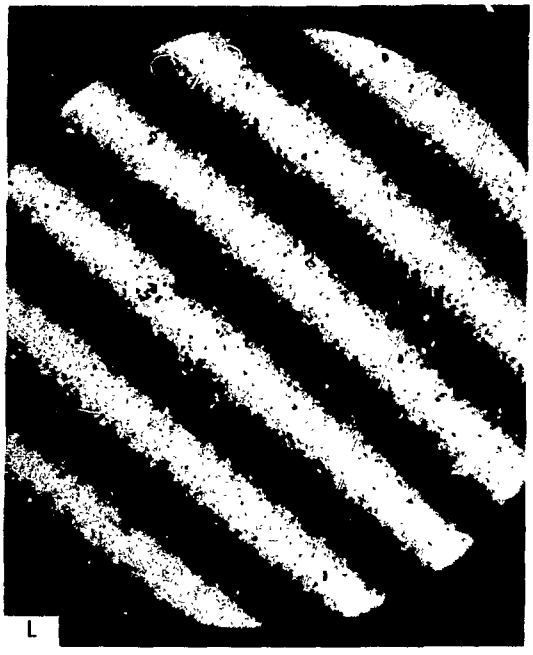
L


M

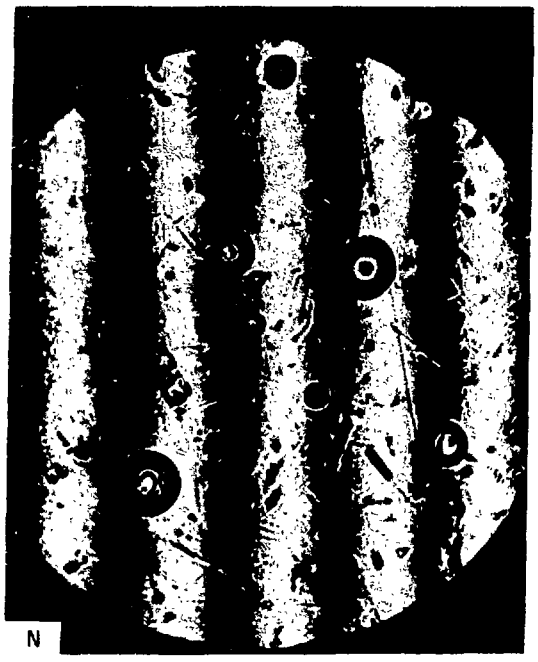
N


O


R

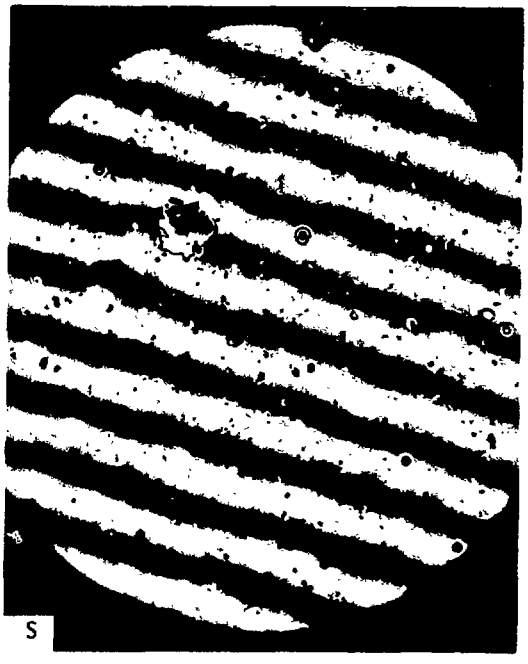
S

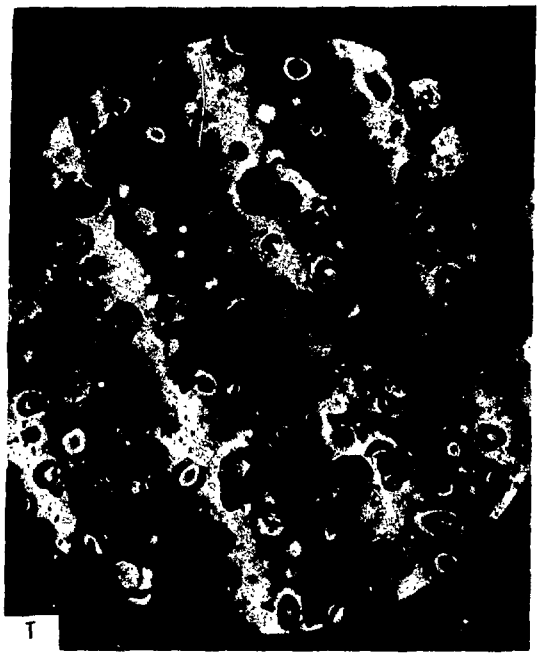

T

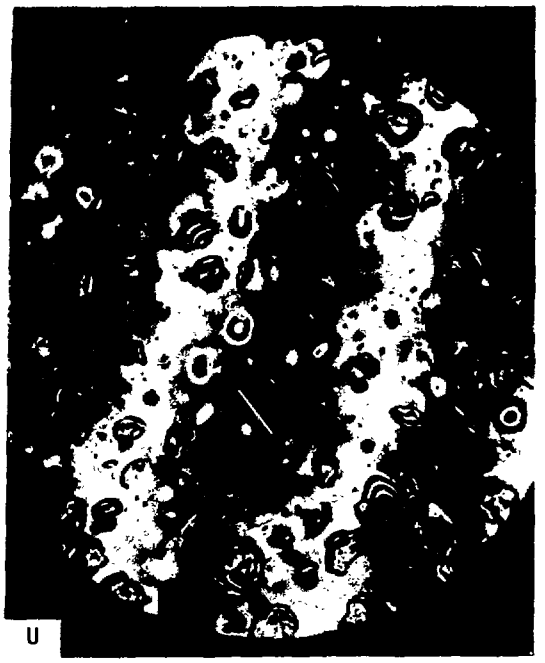

U

V

Fig. 5: Photographs of blisters taken with the Zeiss interference microscope, contour interval 0.27 μ. At magnification 2 (M-2) the circle is 0.73 mm across; at magnification 3 (M-3) the circle is 0.28 mm across; at magnification 1 (M-1) the circle is 1.82 mm across. The dose is given in parentheses in mC/cm^2 following the ion. Unless noted, all ion energies were 140 keV.

A. Spinel M-2 H(60) photographed 12-1/2 years after bombardment;
B. Sapphire M-3 H(60) photographed 12-1/2 years after bombardment.
C. Lucalox M-3 H(144);
D. Lucalox M-3 He(180);
E. Alumina, Ceralloy 138, M-2 H(61);
F. Alumina, Ceralloy 138, M-3 D(137). Note the irregularity of the blister interference bands indicating the blister has formed by coalescence of tiny blisters;
G. Alumina, Ceralloy 138, M-3 He(228) note how irregular the blisters are;
H. Silicon nitride Si_3N_4, Ceralloy 147A, M-3 H(182);
J. Silicon nitride Si_3N_4, Ceralloy 147A, M-3 D(182);
K. Silicon nitride Si_3N_4, Ceralloy 147A, M-3 NOT bombarded;
L. Same bombarded He(182);
M. Silicon carbide, Ceralloy 148I, M-3 H(228);
N. Silicon carbide, Ceralloy 146I, M-3 D(279), the blisters are so high ($\sim$ 4 μ) it is not possible to focus on them and on the base.
O. Silicon carbide, Ceralloy 146I, M-3 He(228);
R. Boron Carbide B_4C, Ceralloy 546, M-2 D(182) delayed blistering and exfoliation near edge of bombarded area;
S. Boron carbide B_4C, Ceralloy 546, M-3 He(137);
T. Titanium boride TiB_2, Ceralloy 225, M-3 H(46);
U. Titanium boride TiB_2, Ceralloy 225, M-3 D(91);
V. Titanium boride TiB_2, Ceralloy 225, M-3 He(137); note secondary and tertiary blistering, primary and secondary blistering.

$$r = (a^2 + \frac{1}{4} L^2)/2a \ ,$$

$$V = \frac{1}{2} \pi a(\frac{1}{3} a^2 + \frac{1}{4} L^2), \quad \text{and}$$

$$\Delta L/L = 2\ a^2/L^2 \ .$$

Since a << L, it follows that:

$$P = 2F/a$$

$$= 0.00156\ D/M, \text{ and}$$

$$Y = \frac{15}{16} PL^2/at$$

$$= 0.00293\ DL^2/M\ a^2t \ ,$$

where all linear dimensions are in microns, P is in atmospheres, F is the gas molecules involved in cm-atmospheres, M is the number of atoms/molecule of gas, D is the dose in 1000 microampere minutes/cm^2, and Y is obtained in psi. Data for the materials studied are given in Table IV.

While many of the values in this table do correspond to elastic moduli of these materials, such blister objects could never form because the rupture moduli are orders of magnitude smaller. Further, it is obvious that such gas pressures do not exist in the blisters because gases at thse pressures would have densities of a solid, refractive indices 1.5--2, and the monochromatic fringes would show orders 1.5--2 times those observed. Therefore, these pressures do not exist, and the mechanism for blister growth must be quite different from the growth of a soap bubble.

THE BLISTERING PROCESS

A pressure parameter can be calculated from the dose and the elevation,

$$P_\ell = 9.64\ D/Mf \ ,$$

where P_ℓ is in psi, D is in mC/cm^2, M as before is the molecularity of the gas, f is the elevation in fringes (in the present case units of 0.27 μ), whose raison d'etre is elevation caused by porosity. The behavior of this parameter with dose could vary greatly with circumstances. If the body were permeable, the parameter would rise steeply with dose. If a radiation expansion were occurring, the parameter would be low. When porosity is developing, the parameter should rise rapidly to a stable value and remain there. The value would be smaller were a lateral deformation occurring. More complicated behavior would be seen were a combination of these circumstances occurring. If blistering were to develop, the parameter might fall sharply. All of these phenomena are seen in the curves of Fig. 6. Yet despite these complicating features, the parameter is seen to have a persistent value of order of magnitude 10^4 psi. Such a value is not unreasonable for the strength of materials. At these pressures, the densities of the gases are

Table IV: Blister calculations.

Material	Ion	Dose (mC/cm^2)	Range (μ)	Diameter (μ)	Height (μ)	r (μ)	$\Delta L/L$ (%)	Calculated V (μ^3)	P (10^4 atmos.)	Y (10^6 psi)
Si_3N_4	H^+	137	1.03	9	0.38	27	0.35	12	19	37
	D^+	182	1.32	3	0.24	4.8	1.3	0.89	19	5.1
	D^+	182	1.32	4	0.27	7.5	0.91	1.7	17	7.3
	He^+	182	0.72	1	0.22	0.69	9.3	0.11	43	2.6
Lucalox	H^+	144	0.9	7.3	0.054	120	0.011	1.13	69	710
	He^+	72	0.56	10.5	0.47	29	0.41	21	7.9	31
	He^+	72	0.56	9.5	0.54	21	0.65	19	6.9	19
	He^+	72	0.56	9	0.43	24	0.46	14	8.7	27
Al_2O_3, Ceralloy	H^+	61	0.9	23	0.50	133	0.094	104	2.5	28
	D^+	137	1.1	31	0.76	160	0.12	290	3.7	4
	He	228	0.56	4	0.30	5.9	5.1	21	8.5	6.1
SiC X1	H^+	364	1.15	15	0.54	52	0.26	48	17	59
	He^+	364	0.93	10	0.81	16	1.31	32	23	39
SiC I	H^+	152	1.14	11.5	0.81	21	0.99	42	4.8	6.5
	H^+	152	1.14	19	1.6	30	1.4	220	2.5	4.7
	D^+	279	1.50	33	4.05	36	3.0	1700	1.7	2.9
	D^+	279	1.50	27	4.3	23	5.1	1200	1.6	1.7
	He^+	152	0.93	5	0.46	7	1.7	4.6	17	9.3
	He^+	152	0.93	4	0.95	2.6	11.0	6.4	8.3	1.4
Sapphire	He^+	36	0.56	10	0.405	31	0.33	16	4.6	19
	H^+	60	0.91	16.5	0.405	84	0.12	43	3.9	27
Spinel	H^+	60	0.94	480	1.7	17000	0.0025	150000	0.92	1200
	H^+	60	0.94	585	1.4	30000	0.0012	190000	1.1	2700
B_4C	H^+	152	1.47	53	7	190	0.26	2100	2.1	19
	He^+	137	0.95	8.4	1.15	29	0.27	8.7	23	52

Table IV (Cont.)

Material	Ion	Dose (mC/cm^2)	Range (μ)	Diameter (μ)	Height (μ)	r (μ)	$\Delta L/L$ (%)	Calculated V (μ^3)	P (10^4 atmos.)	Y (10^6 psi)
ZrO_2	H^+	70	0.91	9	0.95	11	2.2	31	8.2	8
	D^+	70	1.11	40	1.08	12	2.3	43	8.7	6.8
	He^+	46	0.53	12	0.94	19	1.3	54	20	53
	Ne^+	46	0.15	2	0.25	1.8	4.5	0.52	24	20

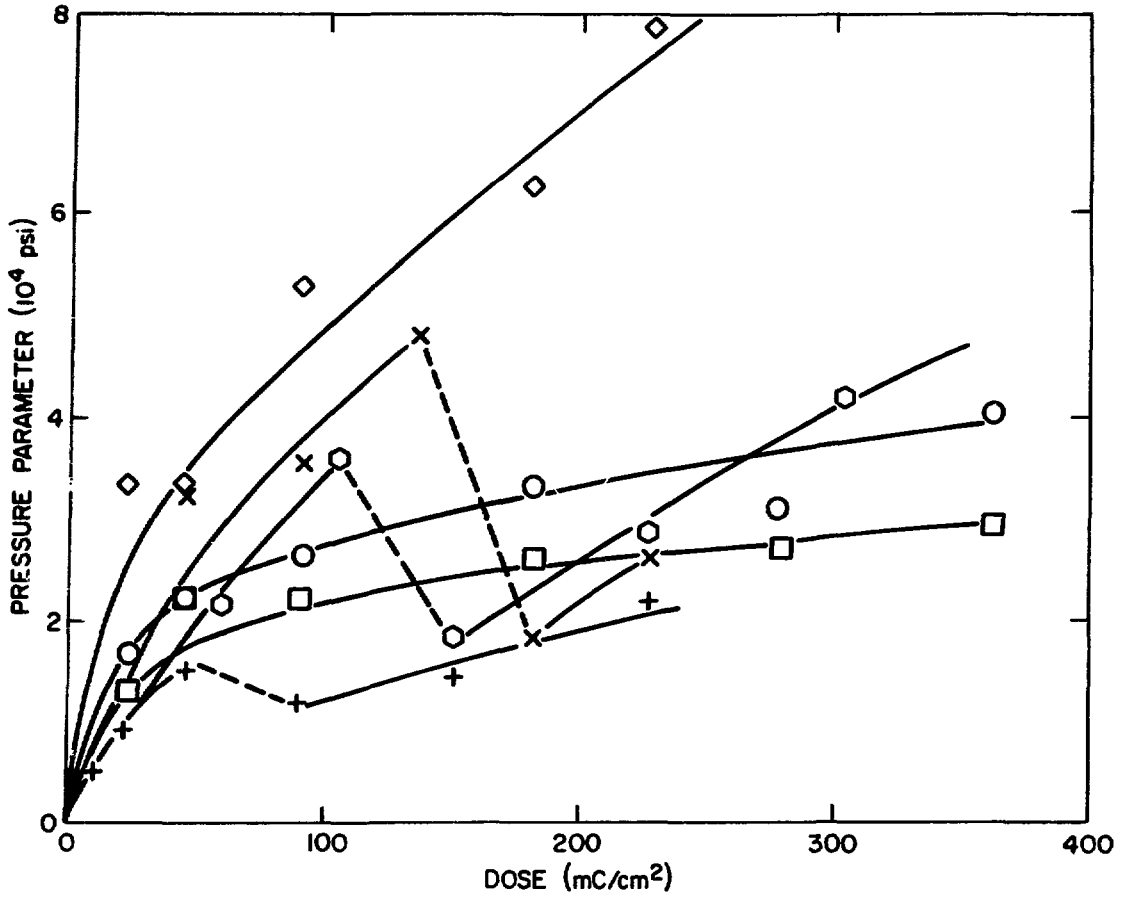

Fig. 6: Pressure parameter P_ℓ as a function of dose for SiC crystals (hexagons H^+ 140 keV, X's D^+ 100, diamonds He^+ 140) and for B_4C compact (Ceralloy 546) (circles H^+ 140 keV, crosses D^+ 140, squares He^+ 140).

less than a tenth that of solids or liquids, hence the refractive index would be close to unity and would not affect the fringe order of the monochromatic fringes appreciably.

The porosity which we are describing cannot be resolved in the optical microscope. This would be under a micron. The elevations which are observed in the early stages of ion bombardment, at 10--20 mC/cm^2, are a small fraction of a fringe, yet these areas show well developed chromatic fringes. This would indicate pores under 0.01 μ at this stage of the bombardment. How would such porosity interact with light whose wavelength is very much longer? It would not behave as a thin gaseous layer in the manner of our previous calculations.[17] Rather, it would behave like a mixed medium of a mean refractive index. As the porosity increased, the effective refractive index would decrease, the effective layer thickness would increase, and the effective shell thickness would decrease. Effects described above for the

behavior of quartz, associated with a non-uniformity of refractive index and density, would be present. However, scattering would be greater than for homogeneous media, reducing reflectivities and introducing damping effects, as would absorbing media. Reflectivities should be greater at longer wavelengths. These effects are seen in the example given here, silicon nitride, shown in Fig. 7. The secondary interference effects (change of fringe amplitudes with wave number) seem to be repressed. When the bombardment is extended, and presumably the pore size is increasing, the fringe amplitude grows markedly more in the intra-red than at lower wavelengths. The reflectivities are much less than would be calculated for homogeneous media.

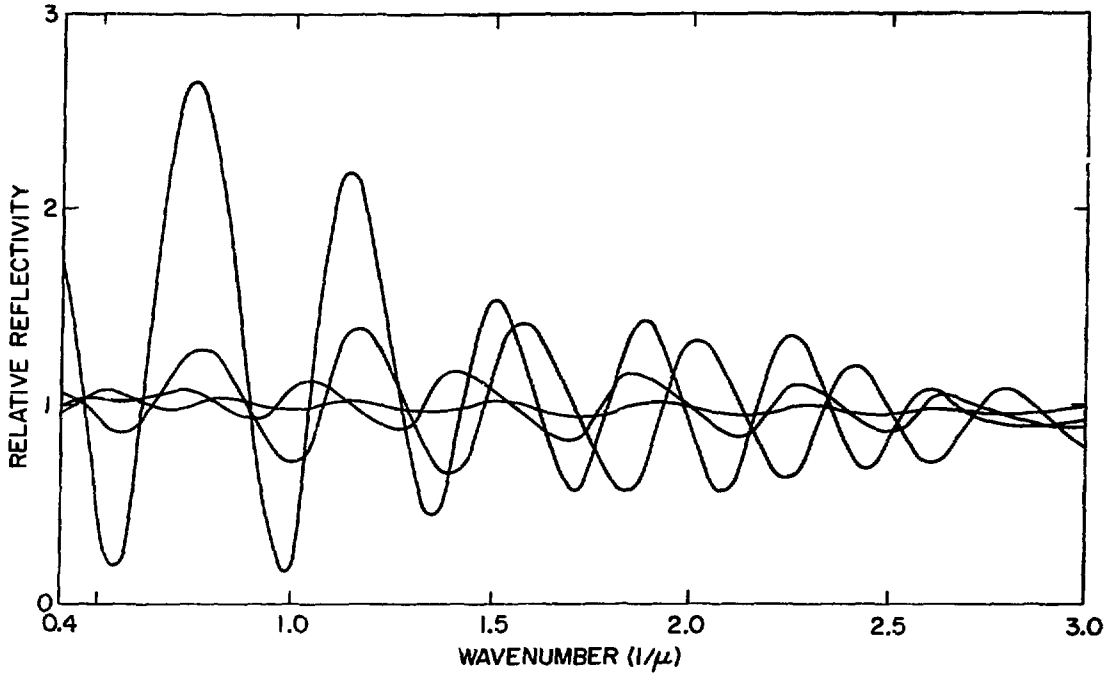

Fig. 7: Reflectivity of He^+ 140 keV bombarded Si_3N_4 compact (Ceralloy 147A) relative to an unbombarded area of the same surface plotted against wave number. The curves in the order of increasing amplitude are for doses 23, 46, 91, and 137 mC/cm^2. The curves for 182 and 228 mC/cm^2 are nearly the same as for 137 mC/cm^2. There is a periodic irregularity in the wavenumber scale which becomes as great as 0.6% of the range shown. Note that for the first 3 doses the optical thickness is increasing.

The process of blister growth was described originally as occurring under the stress of the gas pressure and involving the coalescence of smaller blisters. The micropores may grow under the stress of the gas pressure, but the blistering appears to be quite a different process, a cataclysmic rupture of the porous layer. Even the formation of the smallest

blisters, a few tenths of a fringe high and a few microns in diameter, must cause a dramatic drop in pressure. This drop is readily calculated because the diameter of the blister is much greater than its height. Its volume is therefore about half of the circumscribed cylinder. Such a blister might appear by the time the elevation has reached 0.2 fringes. Thus the pressure would drop to 2/3--1/3 of its former value immediately. This may account for the behavior of the pressure parameter shown for boron carbide in Fig. 6. Formation of blisters a fringe or more in height would cause a pressure drop to a small fraction of its former value. The stretching of the material to form the blister shell would have had to occur prior to the blister formation. It might have been caused by a radiation expansion, or a yielding under stresses developed in the formation of the microporous layer beneath. A shrinkage of the underlying layer could occur with rupturing of the microporous layer and the ensuing pressure drop.

If the internal gas pressure were required for the blister growth, further growth could not take place until the dose were increased several-fold to restore the gas pressure. Blisters, once formed do indeed appear to be stable for a considerable period of further bombardment, but it is suspected that they had grown until some discontinuity of the surface had been reached, that the gas ions dissipate most of their energy in the blister shell, and then the gas can permeate to the surface through imperfections or fissures in the shell. Indeed, most of the larger blisters do show cracks. That other forces are involved in the blister growth is shown by post-irradiation blister formation or growth. An example in the case of sapphire was described earlier.[14] In the present work, the most spectacular case was that of boron carbide shown in Fig. 8. Some of the bombarded layers will exfoliate under stress or shock. Ultrasonic cleaning or even rubbing with soft tissue may be effective. That some of the surfaces which trap gas do not form blisters and that the blisters which develop in the several cases are of various sizes are further evidence that the blisters do not form and grow under the gas pressure, but rather the strains and stresses developed in the surface. In the central portion of a bombarded area of an isotropic medium or in particular directions of a crystal, the stresses are plane. In other directions of a crystal or crystalline material or at the edges of a bombarded area, there are also shear stresses. The importance of shear stresses in the blistering process is shown by blisters often being larger at the edges of a bombarded area, sometimes even in the penumbral area where the dose has fallen off. An excellent example appeared in the bombardment of silicon carbide crystals and is shown in Fig. 9.

SURFACE DEFORMATION AND STRESS RELAXATION

Some of the crystals and crystalline compacts show so little general deformation that the step heights can be determined by assuming the contour of the bombarded area is continuous with the neighboring unbombarded area except for the interposition of a step.[18] In the cases of some of the glasses, it was obvious that the contour of the surface was deformed. An example is shown in Fig. 10. This kind of deformation is not observed with hard crystals (see below) nor is it observed at lower dose with glasses. It therefore cannot be attributed solely to non-uniformity in the ion beam. It may be caused by irregularities in the microporous layer, or it may be caused by the lateral stresses. Where the bombarded layer of a glass has

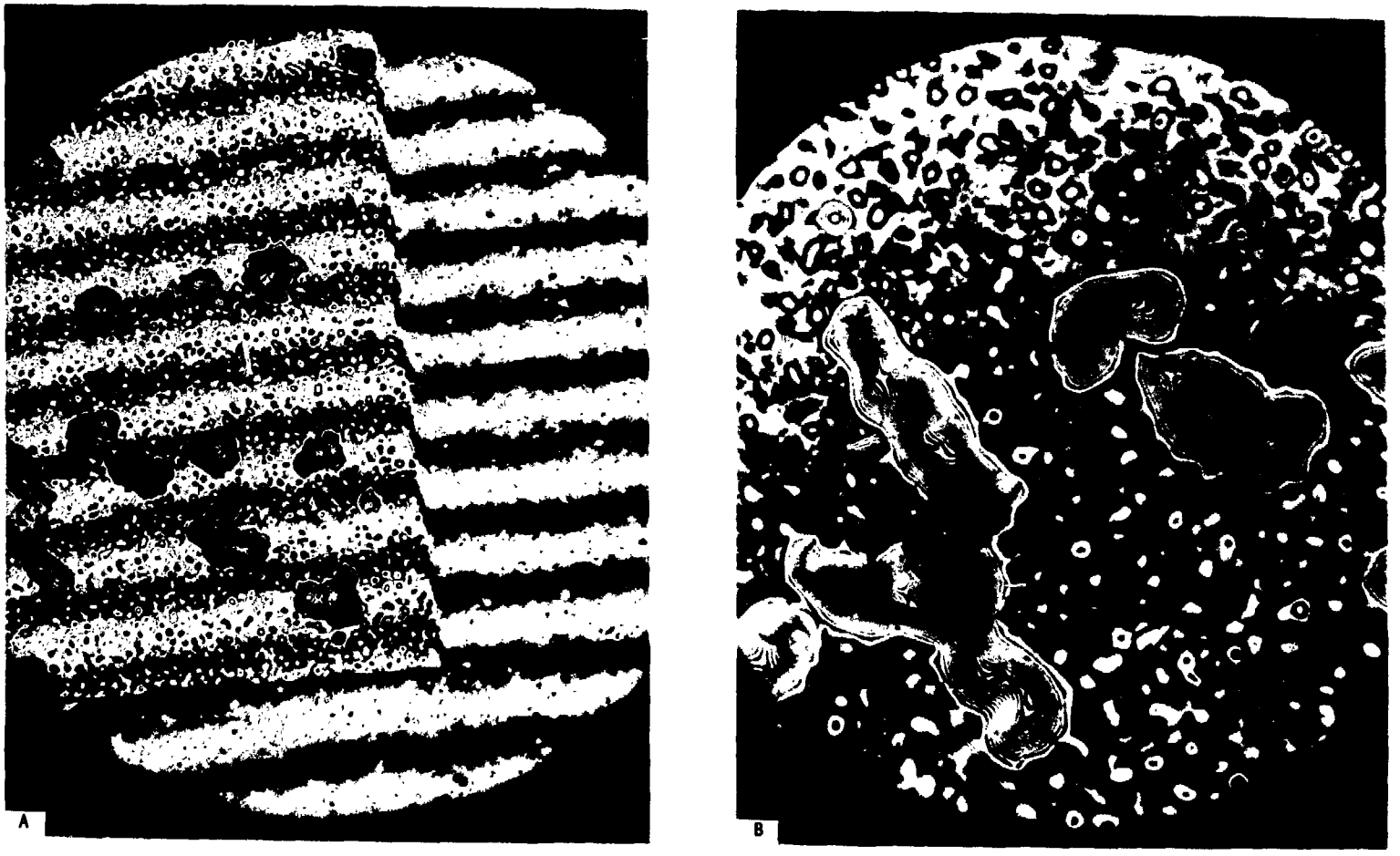

Fig. 8: Microinterferograms of delayed blistering of boron carbide B_4C, Ceralloy 546, H^+ (140 keV), 228 mC/cm², contour interval 0.27 μ. A. Diameter of cricle 1.82 mm; B. Left side of previous picture at higher magnification, diameter of circle 0.72 mm. The large blisters did not appear until several months after bombardment.

Fig. 9: Microinterferogram of part of a silicon carbide crystal bombarded with He^+ (140 keV), 346 mC/cm^2, circle diameter 0.28 mm, fringe contour interval 0.27 μ. Note the large blisters formed at the edge of the bombarded area.

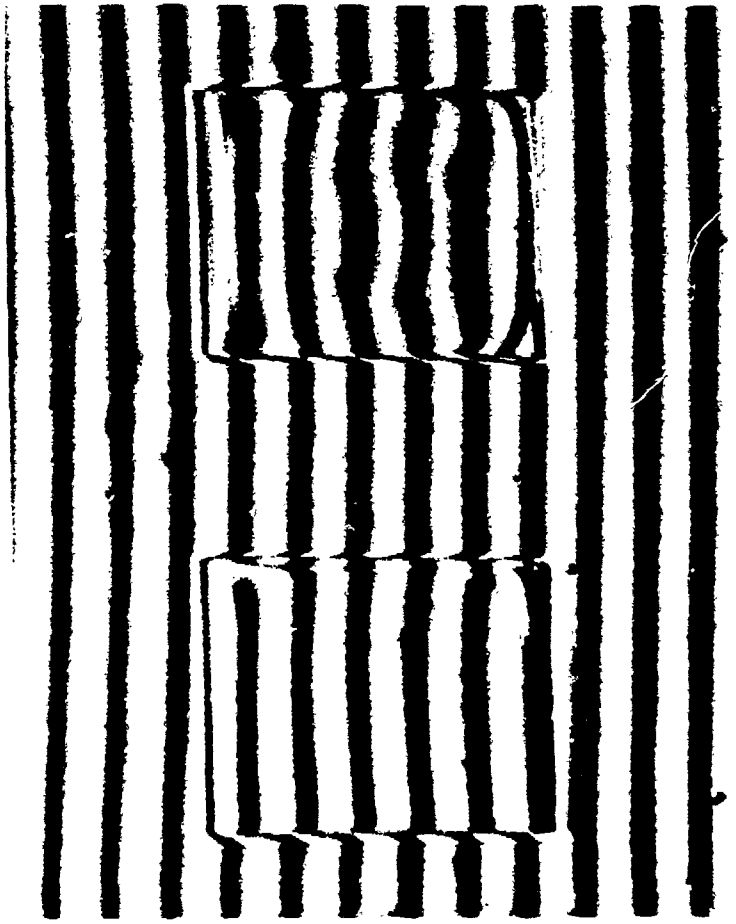

Fig. 10: Interference of light barium crown glass LBC-2 bombarded with 140 keV protons, upper area 182 mC/cm^2, lower area 228 mC/cm^2. The bombarded areas are 2 x 2.5 mm. Note the surface distortion of the bombarded areas.

exfoliated, it has usually been in one of the corners of the bombarded area. These areas have a particularly low reflectivity compared to the exfoliated areas of the crystals. The glasses are a low modulus material compared to the crystalline materials studied here, and they are subject to creep. Therefore the microporosity stage is more prominent and the stresses which give rise to blister formation do not develop. When as in the case of the crown glass, the blisters do develop, they present the appearance of a froth, as if they are the growth of the microporosity rather than resulting from an early fracturing in the microporous layer. This difference in behavior is then attributed to the difference between a high modulus material and one which suffers creep or plastic deformation.

The results of the present study indicate that despite the reflectivity rising above the normal reflectivity during ion bombardment of quartz, there is no evidence of porosity or blistering. Thus it appears that the large elevation found for bombarded quartz areas is caused by extrusion of the total volume expansion. This implies a stress relaxation during ion bombardment as described in an earlier article.[19] The surface contour appears to be preserved in this process. The manner by which this occurs is significant for our understanding of the radiation disordering of crystalline materials. A more intensive study of quartz is planned. Such a stress relaxation appears to be associated with the silica structure since it is found also in vitreous silica. It may therefore be part of the phenomena seen in the ion bombardment of other glasses and may help account for lack of blistering in these materials despite large elevations.

CRAZING

Crazing was first seen in this laboratory in ion bombardment of vitreous silica with ions of energies above a few tenths MeV.[19] This was associated with the radiation-induced compaction. A photograph of this crazing shows the typical polygonal patterns reminiscent of those formed when mud dries.[20] Such crazing is not seen at the lower energies utilized in the present investigations. This was attributed to a plastic flow stress relaxation occurring.[19]

The next example of crazing which was seen in this laboratory was found on ion bombardment of lithium niobate and has been reported.[14] Photographs of this crazing are reproduced here in Fig. 11 because its interpretation must be reconsidered in the light of observations just made of graphite.

When graphite crystals were bombarded with any of the ions, protons, deuterons, or helium, 140 keV, triangular crazing patterns appeared, similar to those found on ion bombarded Z-cut lithium niobate. Examples are shown in Fig. 12. On examination at high magnification, the crazing appears to consist of long narrow blisters. The only reasonable explanation for such an occurrence is the migration of the gas to dislocations where it is trapped. Crystals of this kind of graphite had been studied by Gerhart Hennig and by George Montet. The latter indicated that screw dislocations which had been observed in such graphite crystals would account for the observations (private communication).

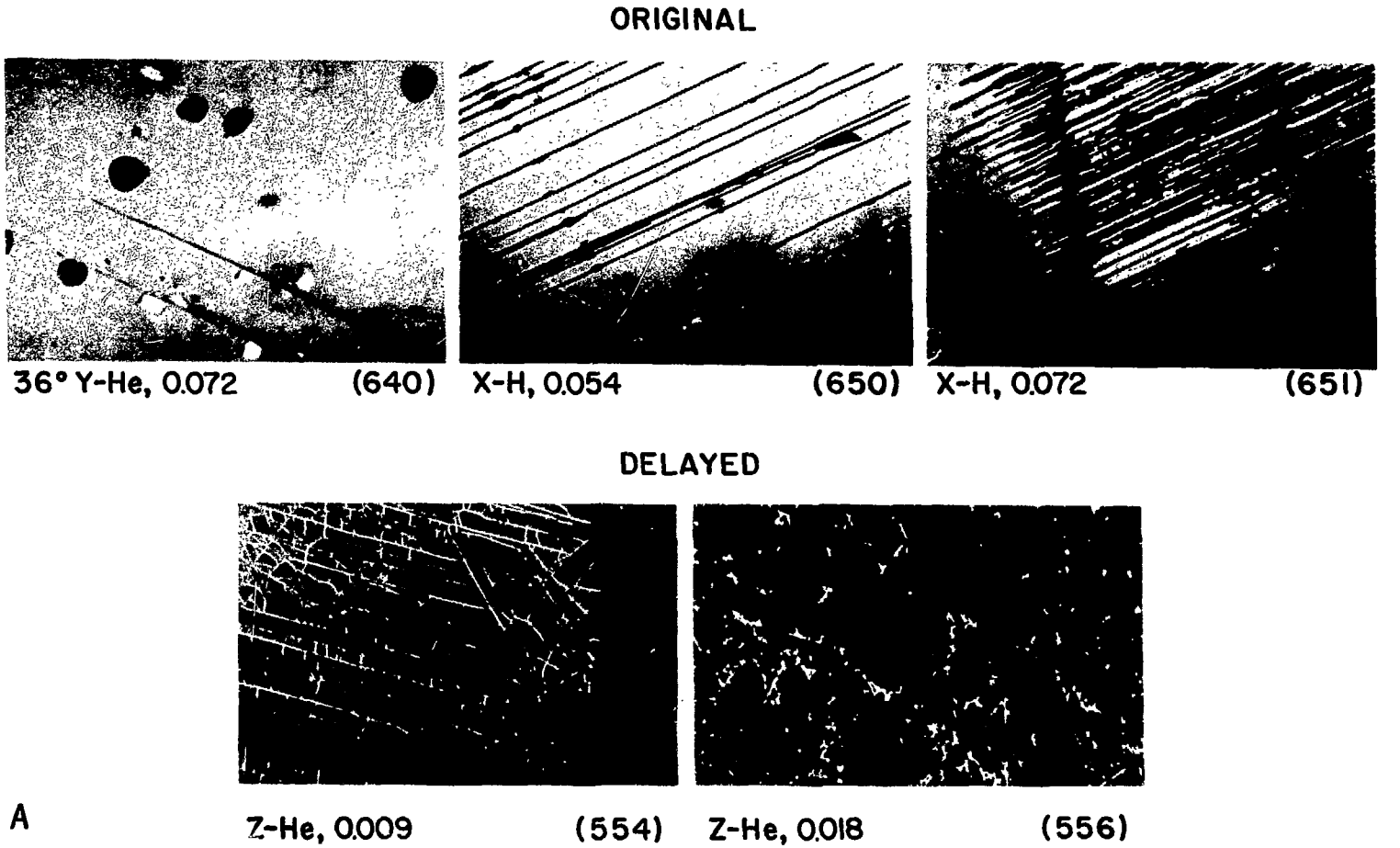

Fig. 11A: Microphotographs of blistering and crazing of ion-bombarded lithium niobate; code is cut, ion, dose (1/2 C/cm^2),(photo-identification number).

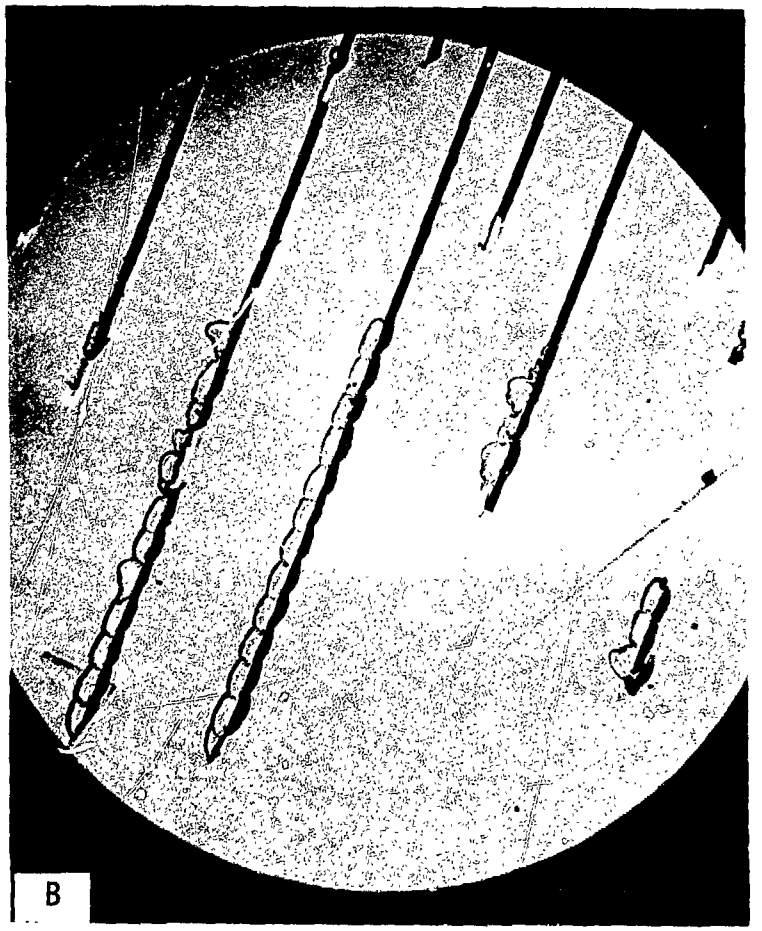

Fig. 11B: The edge of the bombarded area of photo 651 at higher magnification, circle diameter 0.28 mm.

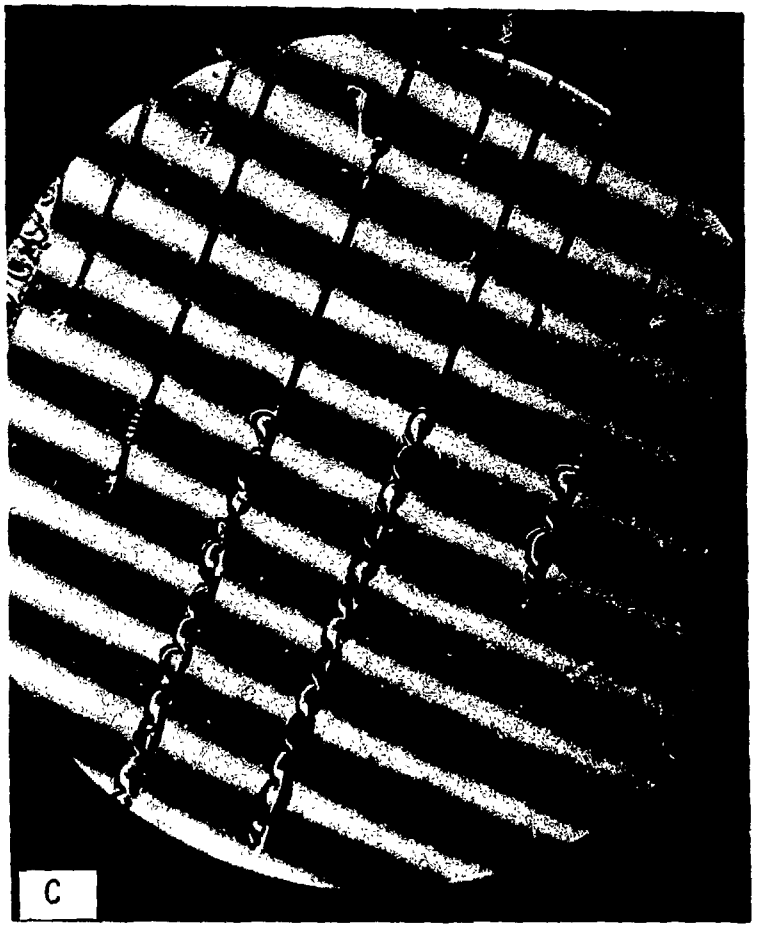

Fig. 11C: The same in interference, contour interval 0.27 μ. The craze fractures appear to consist of elongated blisters.

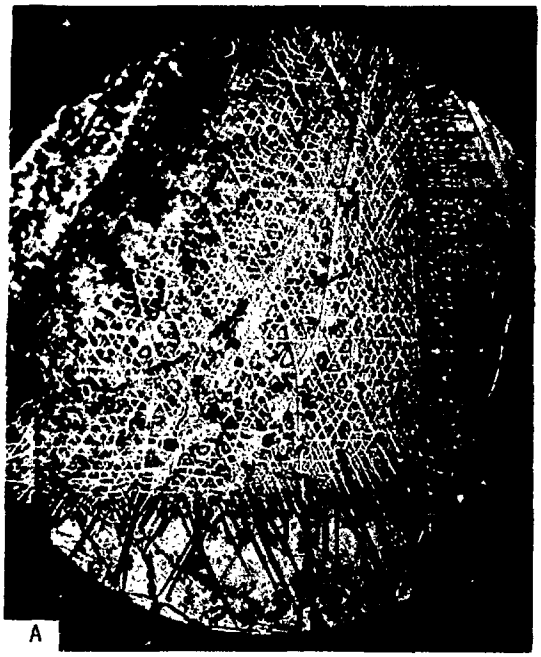

Fig. 12: Ticonderoga natural graphite crystal, photomicrographs of one corner of an area bombarded with He^+ (140 keV) 12 mC/cm^2.

A. No interference, circle diameter 0.73 mm; note darts extending beyond the bombarded area.
B. Same in interference, contour interval 0.27 μ.
C. Corner at higher magnification; circle diameter 0.28 μ; note the darts prove to be elongated blisters.

Some of the parallel crazing observed in the case of lithium niobate has the appearance of narrow furrows and could have been formed by the breaking away of blister shells. The crazing found after storing lithium niobate irradiated with thermal neutrons (tritium and helium generated by lithium fission) showed a series of narrow steps.[21] These could have been formed by the migration of gas to dislocations which then fractured.

It seems likely that interstitial damage becomes trapped at dislocations and makes the material impervious to the gas in this region. The resultant stresses must assist in the precipitation of the gas and the subsequent blistering or fracturing of the crystal.

GROWTH OF CRYSTALS AND COMPACTS

The growth curves for crystals and compacts do not appear to be much different from the growth curves obtained for glasses, some steeper, some less steep, some showing abrupt changes; but when an attempt was made to account for these variations in behavior, it becomes obvious that they possess an individuality and that a variety of mechanisms is involved.

The growth of crystal quartz can be accounted for by the known radiation-induced expansion being manifested vertically; i.e., that material is extruded.

Growth curves for silicon carbide crystals and for compacts are shown in Figs. 13-16 plotted in absolute values and in percentage of the range in the original material. Were the growth caused by porosity, the absolute values would be the more significant; were it caused by a radiation-induced expansion, the percent growth would be more significant. The percent growth is far too great to be accounted for by a radiation-induced expansion. If the growth were just the introduction of porosity, the growth for helium ions should be twice that for hydrogen and deuterium, because the latter form diatomic gases. This is approximately true for the hydrogen and the helium, but the deuterium does not conform. The beams were not entirely uniform, but this will not account for the results, for the extent of the non-uniformity is shown by comparing the second and fifth points on each curve, data for the central area of the beam, with the other points, data from the peripheral area of the beam. Since the hydrogen and deuterium are chemically alike, the differences must be caused by either the energy or the particle deposition, both of which are more uniform along the range for deuterium and helium, and both of which deposit a great deal more energy in the lattice (in contrast to the electronic system). It would thus seem that a radiation-induced creep or stress relaxation, or a lattice transformation may be taking place. The behavior of the compacts can be readily understood as growth occurring in the same manner until channels are established which permit the release of implanted gas through the surface.

A further understanding of the growth phenomena may be obtained from the behavior of boron carbide compacts, curves for which are given in Fig. 17. The fractional percentage growth is a little too large to be attributed to a radiation expansion, but the evidence for porosity shown by the chromatic fringes in the near infra-red makes the case for porosity overwhelming. The data shown in these curves were obtained within a few weeks of

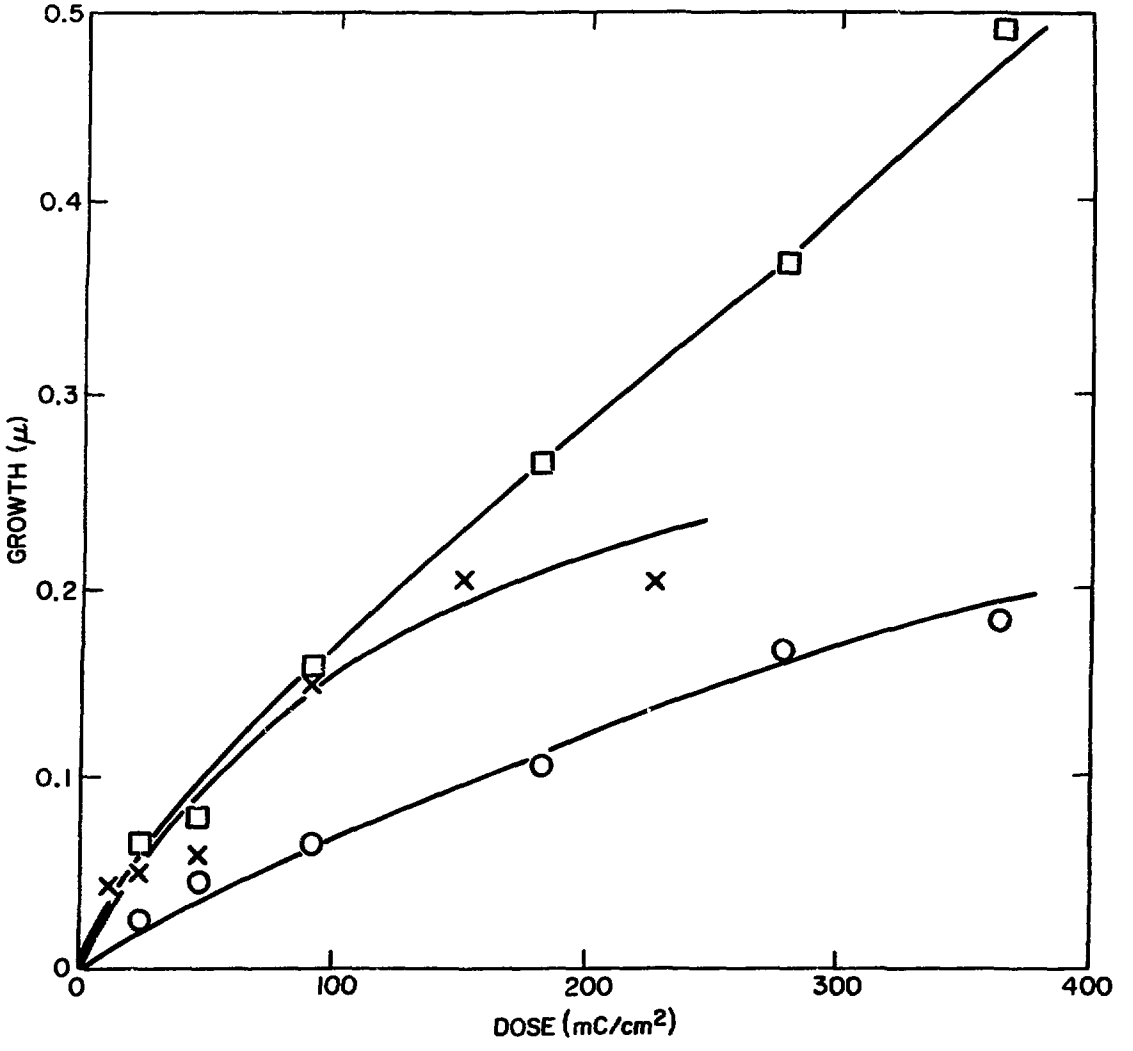

Fig. 13: Absolute growth of single crystal silicon carbide bombarded on the basal plane; squares He^+ 140 keV, X's D^+ 100 keV, circles H^+ 140 keV.

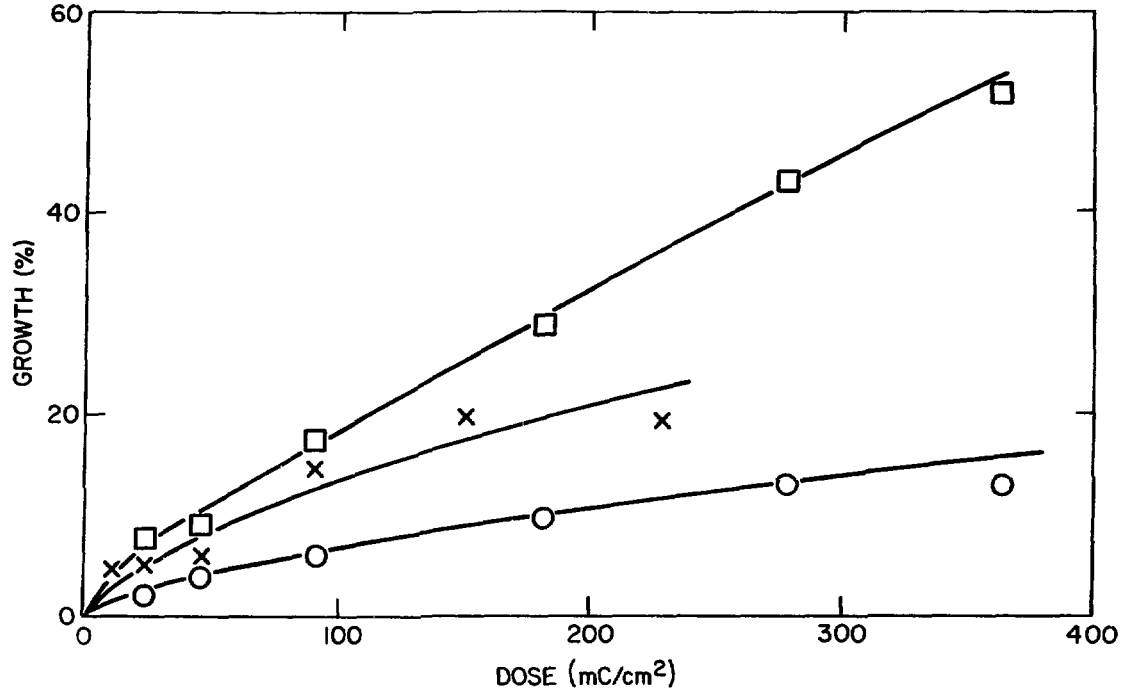

Fig. 14: Same as Fig. 13 except growth given in percent of range.

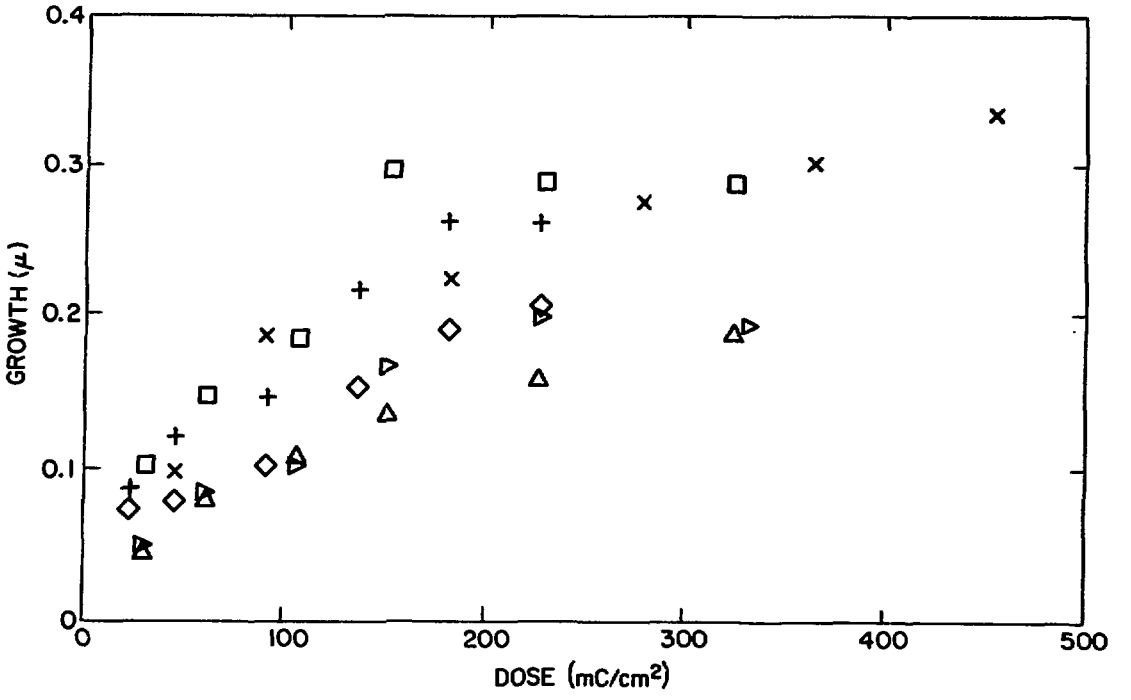

Fig. 15: Absolute growth of silicon carbide compacts: diamonds, crosses, vertical points, "Ceralloy 146A"; squares, X's, horizontal points, "Ceralloy 146I"; diamonds and squares He^+ 140 keV, crosses and X's D^+ 140 keV, arrow points H^+ 140 keV.

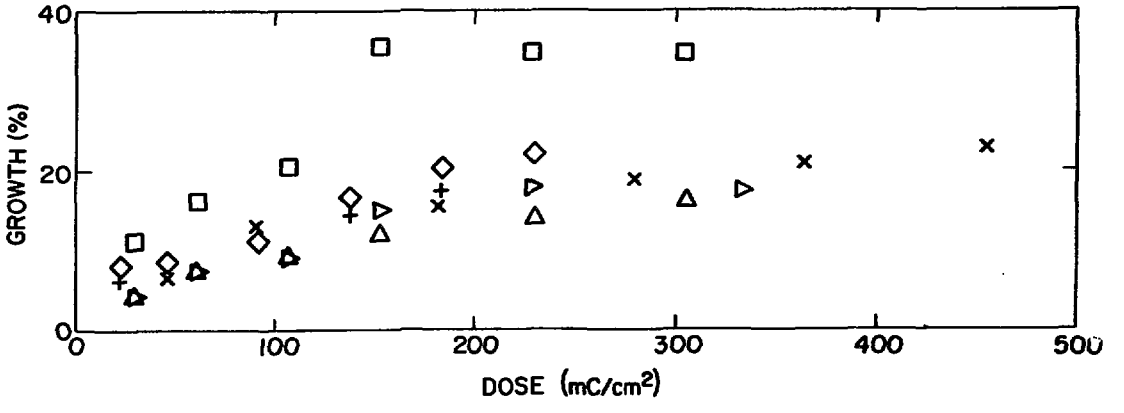

Fig. 16: Same, but growth given in percent of range.

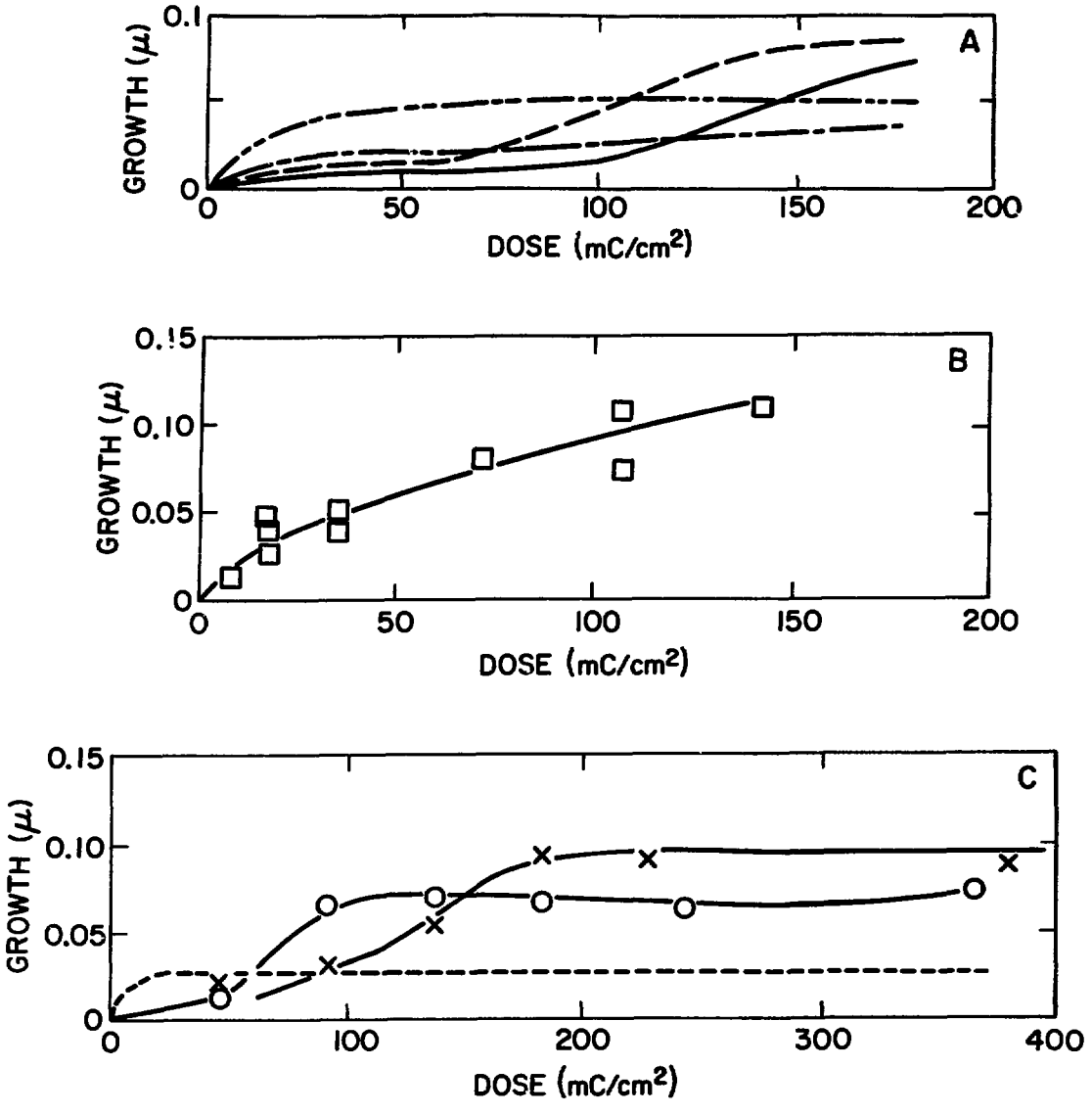

Fig. 17: Growth curves. A. Data for sapphire and Lucalox from earlier investigations in this laboratory; line H^+ 140 keV on sapphire; dashes He^+ 140 keV on sapphire; dash-dot H^+ 140 keV on Lucalox; dash-2 dot He^+ 140 keV on Lucalox. The relative dose rates are nearly as reliable as the present data, but the absolute value is less certain. B. Alsimag 0915 ($BaTiO_3$) bombarded with He^+ 140 keV. C. Magnesia stabilized zirconia; circles H^+ 140 keV; crosses D^+ 140 keV; dashes Ne^+ 140 keV.

At the higher doses, blister formation was seen in the zirconia and aluminas. With He^+ 140 keV the zirconia blistered at all doses; hence, no attempt was made to measure the specimen.

bombardment. They show an abrupt increase in growth for the proton and deuteron bombardments at about 150 mC/cm^2, while the growth on helium ion bombardment is gradual. To begin with, the absolute values of the growth were greater for helium than for hydrogen or deuterium, but after this abrupt increase, the growth was the greater for the latter two. An abrupt rise in the growth curves is usually caused by the fracturing in the microporous layer. That this must have been occurring was indicated by the spontaneous changes which occurred some months later; the areas highly bombarded with protons and deuterons developed the enormous blisters described above. The helium ion bombarded surface is still stable. The gas retention of the boron carbide is not known; but the large rate of growth indicates it to be highly impermeable. The greater stability of the helium ion bombarded surface is therefore attributed to a wider distribution of smaller pores; and there may be a more uniform distribution of radiation damage, if it occurs, along the range.

Growth curves for silicon nitride compact, several forms of aluminum oxide, for magnesia stabilized zicronia, and for barium titanate are given in Figs. 17 and 18. Most of these data were obtained by visual inspection of interferograms rather than by precise measurement and calculation, hence may be subject to minor correction. However, the general character of the behavior is definite. The behavior of these materials are much the same except for evidence of mild breakaway in some of the growth curves. The surfaces rise gradually as porosity in introduced. They then remain relatively stable for long periods of bombardment, and it is presumed that channels for the escape of gas have been established. The curves for the single crystal surfaces (e.g., sapphire) are somewhat deceptive about the stability of the surface, because large areas exfoliated; and the growth curves plotted here are for the part that did not exfoliate.

ABLATION RATE

In all of the studies conducted in this laboratory, several respective areas on a specimen were subjected to ion bombardment to a different dose (see Appendix III). In the original work with single crystal surfaces a progressive increase in the density of blisters was observed; and at the highest dose, exfoliated areas on which blistering had begun anew were seen. On the basis that exfoliation had become prominent between 200 and 400 mC/cm^2 of ions, the ablation rate was given as roughly 1/4 atom per incident ion.[20] In the present study, it has become obvious that there is no definite dose for the breaking away of blister shells. In some cases the blister shells endured for a dose an order of magnitude greater than that at which the blisters developed. Thus it would seem possible to develop surfaces in which porosity may develop and some blistering may occur, but the blister shells would dissipate the energy of the ions and the gas would escape. Although the ablation rate would be greatly reduced, the surface would yet deteriorate if porosity developed. The only way to prevent this from occurring would be to use a material permeable to the gas.

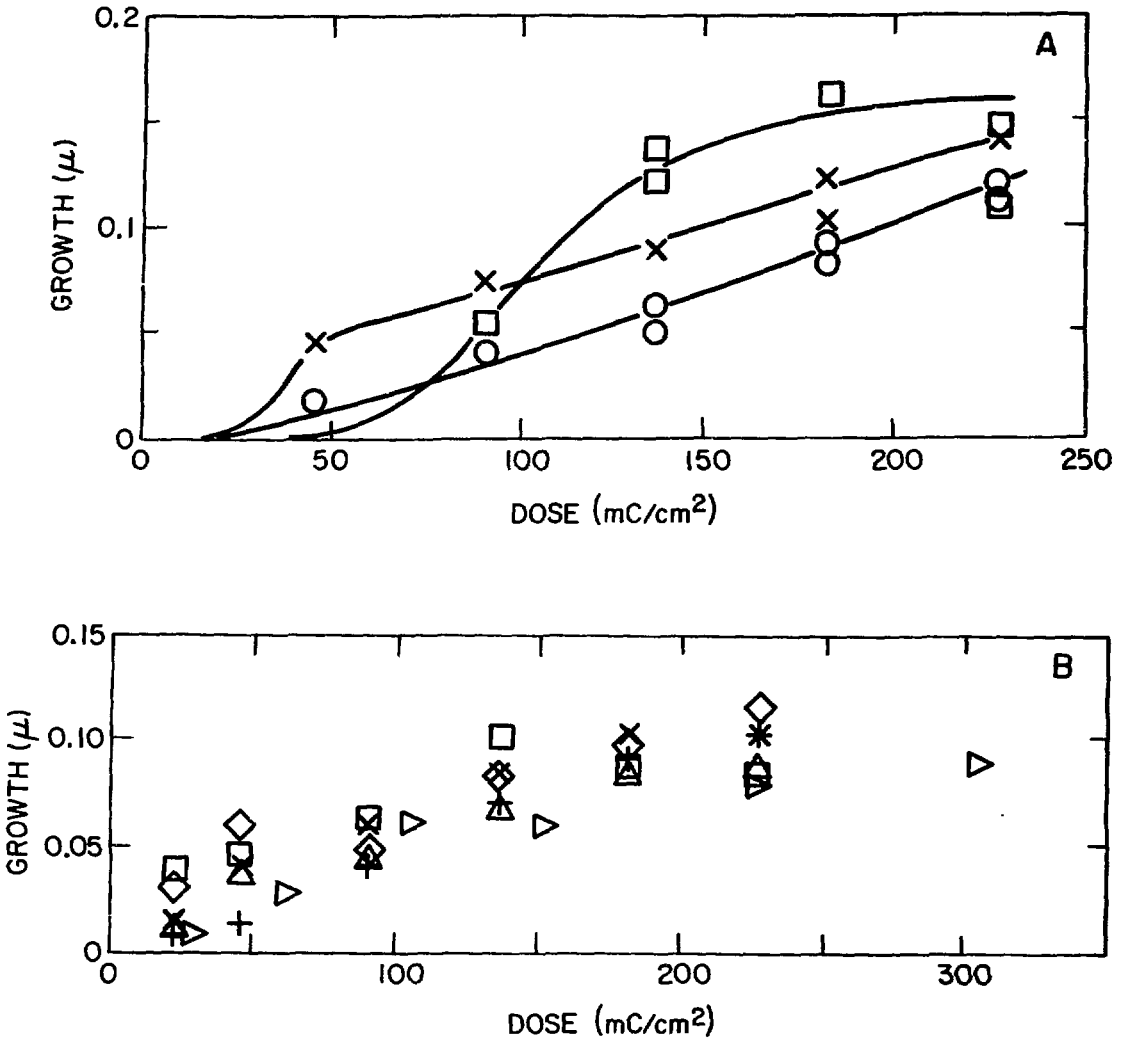

Fig. 18: Growth curves for 140 keV ion bombardment; circles or arrow points H^+, crosses or X's D^+, squares or diamonds He^+. A. Si_3N_4 compacts. B. Alumina: horizontal arrow points, crosses, and squares, Ceralloy 138; vertical arrow points, X's, and diamonds, Coors.

APPENDIX I: MATERIALS

Single crystal sapphire and spinel used in the original studies[9] were obtained from Linde Products Co. in the late 50's and early 60's. These materials do not correspond to presently available material because crystal growing procedures have been altered. The magnorite crystals were obtained from a secondary source, Semi-Elements, Inc., and became unavailable in the midst of that investigation.[17]

In the present studies, the glasses were commerical glasses on hand in our optical workshop. A number of these had been purchased from Hayward Optical Co. and are no longer available. However, similar glasses are available from other sources. Glasses, even from the same source, will vary in composition from batch to batch because the optical industry is usually concerned only with obtaining particular values of refractive index and dispersion, and additives are used to adjust these values in the melt rather than carefully controlling composition, which seems more difficult. The Si_3N_4, SiC, B_4C, TiB_2, and Ceralloy alumina compacts were obtained from Ceradyne, Inc. The Coors alumina was supplied by F. W. Clinard (LASL). The Lucalox was a gift from the General Electric Co. The ZrO_2 was composition 1859, magnesia stabilized, and was a gift from Corhart Refractories Co. The barium titanate was Alsimag 0915, a gift from the American Lava Corp. The SiC crystals were from a small group of crystals given to us by T. J. Neubert in the late 1940's. Only three of these crystals were large enough for the present studies. Other crystals from this group had been used in an earlier study of radiation effects in silicon carbide.[4]

The glasses were lapped and polished by customary optical workshop procedures. The other materials were finished with successively finer grades of diamond compound.

The graphite crystals were obtained from Ward's Natural Science Establishment in the late 1940's and were identified as having been collected in the Ticonderoga, New York, area. These crystals are much larger and much less perfect than the crystals reported on in our papers on the electrical conductivity of graphite and which had been collected by ourselves in that area.

APPENDIX II: BOMBARDMENT PROCEDURE

Specimens were subjected to ion bombardment with 140 keV ions (except for one SiC crystal which was bombarded with 100 keV deuterons) produced with a Cockcroft-Walton accelerator and then analyzed. Ion bombardment was through a mask arrangement which permitted placement of 6 areas 80 x 100 mils, each of different dose, in the length of time required to obtain the greatest dose, each spot being masked off at the appropriate dose. The masks did not maintain registry as they were moved, giving a set of small steps about the areas receiving higher dose. The penumbral effect was small. The convenience of this masking arrangement was obtained at the sacrifice of a loss of precision in the dose, because the beam was not stable over the period of these long bombardments. The accumulated charge was read with instrumentation whose precision was estimated as a few per cent, and the current was calibrated against that received by a Faraday cup substituted for the specimen; but the precision of the charge incident on the bombarded areas may have been poorer than 20% because of beam instability and non-uniformity.

In earlier work, the target was kept at ground potential; and it was not understood that the charge accumulated on an insulator would greatly affect the secondary emission. Prior to the present studies, the secondary emission from the target holder was investigated carefully,[22] and it was found that currents, practically the same as those obtained in a Faraday cup, could be obtained by biasing the target structure 30-70 v positively with respect to the surrounding structure. A defining aperture (used to define the beam area) is also biased positively to prevent its secondary electron emission from entering the beam.

APPENDIX III: EXPERIMENTAL PROCEDURES

Specimens were examined first with an American Optical Co. microscope fitted with a vertical illuminator illuminated by a Bausch and Lomb monochromator 33-86-25. Most of the photographs taken with this instrument were made with a Nikon microflex unit to which a 35 mm camera body was affixed. Reflectivity determinations or spectra covering the range 0.4 to 0.75 μ could be made with this unit. A potentiometer transducer was affixed to the monochromator. On the camera tube was mounted a Photovolt photomultiplier photometer (F-unit). The data were plotted on a Houston X-Y recorder. Reflectance spectra covering a greater wavelength range were obtained with a special fixture mounted in the sample compartment of the Beckman DK-2A spectrophotometer. Spherical mirrors were used to focus a small aperture on the specimen and to project the reflected light on the detector. In the first unit made, an aluminum mirror was used in the reference beam. It proved unsatisfactory because of an inverse peak in the reflectivity of aluminum at about 0.9 μ. In the second unit, lithium niobate was used in the reference arm and proved more satisfactory. Both, the spectra from microscope and the spectra from the spectrophotometer, were rectified by digitizing the curves obtained from the respective X-Y plotters at irregular intervals, transforming the resultant data suitably, and then interpolating over short overlapping intervals by second order least squares polynomials to obtain a 170 point data set spaced uniformly in the independent variable over the range of interest.

Interferograms of the specimens as a whole were obtained with a Twyman-Green interferometer based on a Gaertner Michelson interferometer. The photographs were made with a Nikon microflex unit on 35 mm Tri-X film which was processed with Edwal Super-20. These were enlarged to about 4 x 5 inches. Some of the films were read visually with the aid of scales. When more precise determinations of step heights were required, the prints were read with a scanner,[18] the data were transferred to paper tape by means of a data logger, and the contours were calculated by Emerson's method.[23] Particularly in the cases of the glasses, the bombardment deformed the figure of the surface. For this reason, the elevations were obtained by extrapolating the surface contours of the irradiated and the unirradiated areas into the intermediate region by least squares fits, usually a linear one, but in extreme cases by a second order fit.

Microinterferograms were made with a Zeiss interference microscope (based on a Twyman-Green arrangement) on Tri-X film. This was usually processed with Edwal FG-7 and enlarged to several inches in diameter. The height of steps shown in these prints were usually read with the aid of a scale. The Zeiss instrument was used visually to obtain blister heights and diameters, and typical examples were photographed.

Refractive indices of the glasses were determined with a Zeiss refractometer Model A. For the opaque crystals, the optical constants were determined from the principle angle and azimuth of reflected circularly polarized light as determined with a Gaertner ellipsometer.

REFERENCES

1. W. Primak and L. H. Fuchs, Phys. Rev. 103, 541 (1956).
2. W. Primak and L. H. Fuchs, Nucl. Sci. Eng. 2, 49 (1957).
3. E. Primak, Phys. Rev. 103, 1184 (1956).
4. W. Primak, Radiation Effects on Silicon Carbide (Pergamon Press, N.Y., 1960), p. 385.
5. W. Primak, Phys. Rev. 95, 837 (1954).
6. W. Primak, Nucl. Sci. Eng. 2, 117 (1957).
7. The use of accelerators for such studies was demonstrated by R. L. Hines, Phys. Rev. 100, 1267 (1955).
8. W. Primak, Y. Dayal, and E. Edwards, J. Appl. Phys. 34, 827 (1963).
9. W. Primak, J. Appl. Phys. 34, 3630 (1963).
10. W. Primak, J. Electrochem. Soc. 12, 1002 (1975).
11. R. L. Hines, J. Appl. Phys. 28, 587 (1957).
12. W. Primak, Electrets, Charge Storage and Transport, Electrochemical Soc., p. 546 (1973).
13. W. Primak, Nucl. Methods 127, 21 (1975).
14. W. Primak, J. Appl. Phys. 43, 4927 (1972).
15. R. L. Hines and R. Arndt, Phys. Rev. 119, 623 (1960).
16. W. Primak, Phys. Rev. 110, 1240 (1958).
17. W. Primak and J. Luthra, J. Appl. Phys. 37, 2287 (1966).
18. W. Primak, Appl. Optics 12, 2894 (1973).
19. W. Primak, J. Appl. Phys. 35, 1342 (1964).
20. W. Primak, J. Nucl. Materials 53, 238 (1974).
21. W. Primak, Nucl. Appl., February 1976 (in press).
22. W. Primak, Bull. Am. Phys. Soc. 19, 31 (1974).
23. W. B. Emerson, J. Res. Natl. Bur. Std. 49, 241 (1952).